ANESTHESIOLOGY

Isoflurane Disrupts Postsynaptic Density-95 Protein Interactions Causing Neuronal Synapse Loss and Cognitive Impairment in Juvenile Mice *via* Canonical NO-mediated Protein Kinase-G Signaling

Swati Agarwal, Ph.D., Michele L. Schaefer, Ph.D., Caroline Krall, B.V.M.&S., M.Sc., Roger A. Johns, M.D., M.H.S., Ph.D.

Anesthesiology 2022; 137:212–31

EDITOR'S PERSPECTIVE

What We Already Know about This Topic

- The PDZ2 domain of the postsynaptic density-95 protein clusters together ion channels and downstream signal transduction proteins at synapses
- Inhalational anesthetics disrupt PDZ2 domain–mediated protein–protein interactions resulting in impaired synaptogenesis and *N*-methyl-D-aspartate receptor–dependent synaptic plasticity
- The downstream signaling pathways linking the PDZ2 domain to synaptogenesis and synaptic plasticity and their response to anesthetics are incompletely understood

What This Article Tells Us That Is New

- In neonatal mice, a 4-h-long exposure to isoflurane disrupted the interactions between the NR2A/2B subunits of the *N*-methyl-D-aspartate receptor and the PDZ2 domain of the postsynaptic density-95 protein
- This disruption led to a decrease in cyclic guanosine monophosphate–dependent protein kinase activity, to impaired synaptogenesis, and to persistent cognitive dysfunction
- *In vivo* and *in vitro* experiments using pharmacologic activators and inhibitors revealed that activation of protein kinase-G by components of the NO signaling pathway constitute downstream signaling mechanisms that prevent these effects

ABSTRACT

Background: Inhalational anesthetics are known to disrupt PDZ2 domain–mediated protein–protein interactions of the postsynaptic density (PSD)-95 protein. The aim of this study is to investigate the underlying mechanisms in response to early isoflurane exposure on synaptic PSD-95 PDZ2 domain disruption that altered spine densities and cognitive function. The authors hypothesized that activation of protein kinase-G by the components of nitric oxide (NO) signaling pathway constitutes a mechanism that prevents loss of early dendritic spines and synapse in neurons and cognitive impairment in mice in response to disruption of PDZ2 domain of the PSD-95 protein.

Methods: Postnatal day 7 mice were exposed to 1.5% isoflurane for 4 h or injected with 8 mg/kg active PSD-95 wild-type PDZ2 peptide or soluble guanylyl cyclase activator YC-1 along with their respective controls. Primary neurons at 7 days *in vitro* were exposed to isoflurane or PSD-95 wild-type PDZ2 peptide for 4 h. Coimmunoprecipitation, spine density, synapses, cyclic guanosine monophosphate–dependent protein kinase activity, and novel object recognition memory were assessed.

Results: Exposure of isoflurane or PSD-95 wild-type PDZ2 peptide relative to controls causes the following. First, there is a decrease in PSD-95 coimmunoprecipitate relative to *N*-methyl-D-aspartate receptor subunits NR2A and NR2B precipitate (mean ± SD [in percentage of control]: isoflurane, 54.73 ± 16.52, $P = 0.001$; and PSD-95 wild-type PDZ2 peptide, 51.32 ± 12.93, $P = 0.001$). Second, there is a loss in spine density (mean ± SD [spine density per 10 μm]: control, 5.28 ± 0.56 *vs.* isoflurane, 2.23 ± 0.67, $P < 0.0001$; and PSD-95 mutant PDZ2 peptide, 4.74 ± 0.94 *vs.* PSD-95 wild-type PDZ2 peptide, 1.47 ± 0.87, $P < 0.001$) and a decrease in synaptic puncta (mean ± SD [in percentage of control]: isoflurane, 41.1 ± 14.38, $P = 0.001$; and PSD-95 wild-type PDZ2 peptide, 50.49 ± 14.31, $P < 0.001$). NO donor or cyclic guanosine monophosphate analog prevents the spines and synapse loss and decline in the cyclic guanosine monophosphate–dependent protein kinase activity, but this prevention was blocked by soluble guanylyl cyclase or protein kinase-G inhibitors in primary neurons. Third, there were deficits in object recognition at 5 weeks (mean ± SD [recognition index]: male, control, 64.08 ± 10.57 *vs.* isoflurane, 48.49 ± 13.41, $P = 0.001$, $n = 60$; and female, control, 67.13 ± 11.17 *vs.* isoflurane, 53.76 ± 6.64, $P = 0.003$, n = 58). Isoflurane-induced impairment in recognition memory was preventable by the introduction of YC-1.

Conclusions: Activation of soluble guanylyl cyclase or protein kinase-G prevents isoflurane or PSD-95 wild-type PDZ2 peptide–induced loss of dendritic spines and synapse. Prevention of recognition memory with YC-1, a NO-independent activator of guanylyl cyclase, supports a role for the soluble guanylyl cyclase mediated protein kinase-G signaling in countering the effects of isoflurane-induced cognitive impairment.

(ANESTHESIOLOGY 2022; 137:212–31)

This article is featured in "This Month in Anesthesiology," page A1. This article has a visual abstract available in the online version.

Submitted for publication February 24, 2021. Accepted for publication April 25, 2022. Published online first on May 3, 2022.

Swati Agarwal, Ph.D.: Department of Anesthesiology and Critical Care Medicine, Johns Hopkins University, Baltimore, Maryland.

Michele L. Schaefer, Ph.D.: Department of Anesthesiology and Critical Care Medicine, Johns Hopkins University, Baltimore, Maryland.

Caroline Krall, B.V.M.&S., M.Sc.: Department of Anesthesiology and Critical Care Medicine, Johns Hopkins University, Baltimore, Maryland.

Roger A. Johns, M.D., M.H.S., Ph.D.: Department of Anesthesiology and Critical Care Medicine, Johns Hopkins University, Baltimore, Maryland.

 Anesthesiology 2022; 137:212–31. DOI: 10.1097/ALN.0000000000004264

Preclinical evidence has raised concerns regarding early neonatal exposures to anesthesia and its effect on brain neurologic functions.[1–4] Animal studies, including those in nonhuman primates, have shown that anesthetic exposure during the neonatal and infant periods results in long-term cognitive dysfunction and impaired neurocognitive performance.[1,5–8] The epidemiologic and animal studies also suggest that exposure to anesthetic agents during early postnatal development may lead to long-term cognitive impairments.[9,10] However, the mechanisms underlying these neurologic deficits are largely unknown. Therefore, it is important to ascertain the cellular and molecular mechanisms that are impaired in response to anesthetic exposures and that produce adverse neurodevelopmental outcomes, including attention deficit disorders and learning and memory impairments.

Several ion channels and receptors at both synaptic and extrasynaptic sites have been highlighted as important targets for anesthetics.[11–13] Many of these ion channels and receptors are associated with their downstream signaling pathways through PDZ domain–mediated protein–protein interactions.[14,15] Our laboratory previously showed that PDZ domain–mediated protein interactions are disrupted by inhalational anesthetics.[15,16] Clinically relevant concentrations of inhalational anesthetics dose-dependently and specifically inhibit PDZ2 domain–mediated protein–protein interactions between postsynaptic density (PSD) protein-95 or PSD-93 and *N*-methyl-D-aspartate (NMDA) receptor (NMDAR) or neuronal NO synthase (nNOS).[15,16] To mimic the action of isoflurane anesthesia, we have used active PSD-95 wild-type PDZ2 peptides, which disrupt PSD–PDZ2—mediated protein interactions by binding to interaction partners.[17–19] This disruption significantly reduced minimum alveolar anesthetic concentration and righting reflex EC50, suggesting that this domain and protein are crucial for anesthetic action.[19] PSD-95–PDZ2 interaction with NMDAR promotes plasticity of excitatory synapses.[20] The multi-innervated spine formation and synaptogenesis are prevented by deletion of the PDZ2 domain of PSD-95.[21] However, the underlying signaling pathways associated with loss of PSD-95–PDZ2 domain—mediated protein interactions and disruption of the PSD-95–NMDAR–nNOS complex in the neonatal hippocampus are unclear. Therefore, we investigated whether clinically relevant concentrations of isoflurane disrupt the PDZ2 domain–mediated protein interaction between NR2A/2B and PSD-95 in the hippocampus of the neonatal mouse brain and underlying mechanisms in primary hippocampal neurons.

Moreover, we examined the effect of isoflurane and PSD-95 wild-type PDZ2 peptide on the dendritic spines and synapse, which play decisive roles in brain plasticity. Spine pathologies are associated with multiple neurologic dysfunctions,[22] and anesthetic agents have been shown to affect spinogenesis and synaptogenesis during the critical period of brain development in rodents.[23–25] We have previously reported that NO donor administration at the time of isoflurane or PSD-95 wild-type PDZ2 peptide exposure helps to prevent synaptic plasticity and memory.[17,18] However, NO interactions with downstream effector molecules and the underlying signaling cascade are unknown and potentially complex. Therefore, in current study, we have used pharmacologic activators and inhibitors to explore each step of the NO-guanylate-cyclase–protein kinase-G (PKG) signaling pathway. Specifically, we tested whether activation of soluble guanylyl cyclase (sGC) by NO or YC-1 is specific and sufficient to prevent isoflurane or PSD-95 wild-type PDZ2 peptides–induced loss in spine density or synapses. Additionally, we tested whether activation of PKG by cyclic guanosine monophosphate (cGMP) analog prevents isoflurane- or PSD-95 wild-type PDZ2 peptide–induced loss of dendritic spines and synapses. To exactly determine the involvement of the sGC-dependent cGMP-PKG signaling pathway, we have introduced the NO-independent sGC activator YC-1 at the time of isoflurane anesthesia in mice to test if cognitive impairments are preventable by sGC activator alone.

Materials and Methods

Materials

Neurobasal media (21103-049), B-27 supplement (17504-044), penicillin and streptomycin (15140-122), Hank's Balanced Salt Solution (4185-052), N-(2-hydroxyethyl) piperazine-N'-2-ethanesulfonic acid (15630080), glucose (A24940-01), horse serum (26050-088), and phosphate-buffered saline were obtained from Gibco (USA). Cytosine arabinoside (C6645), 8-bromoguanosine 3′,5′-cyclic monophosphate sodium salt (8-Br–cGMP [B1381]), 3-(5'-hydroxymethyl-2'-furyl)-1-benzyl indazole (YC-1 [Y102]), laminin (L2020), poly-D-lysine hydrobromide (P6407), bovine serum albumin, and paraformaldehyde were from Sigma-Aldrich (USA). DETA NONOate (82120) was from Cayman Chemicals (USA). 1H-[1,2,4] oxadiazolo[4,3-a]quinoxalin-1-1 (ODQ [0880]) and KT5823 (1289) were from Tocris Bioscience (United Kingdom). The Papain Dissociation kit (LK003150) was obtained from Worthington (USA). Anti-drebrin (ab11068) and Anti-synaptophysin (ab32594) antibodies were from Abcam (USA). microtubule-associated protein-2 (MAP-2; AB15452) and anti-NMDAR2A&B (AB1548) were from Millipore (USA). Mouse monoclonal antibody to PSD-95 (cat. 75-028) was from Antibodies Incorporated (USA) and anti-rabbit and anti-mouse horseradish peroxidase–conjugated secondary antibodies were purchased from Jackson ImmunoResearch Laboratories (USA). GG-12-1.5-Laminin–coated German coverslips were from Neuvitro Corporation (USA). Protein ladder, Alexa Fluor 568 (anti-rabbit) and 488 (anti-chicken), and ProLong Diamond Antifade Mountant (P36961) were purchased from Invitrogen (USA). VECTASHIELD antifade

mounting medium with 4′,6-diamidino-2-phenylindole (H-1200-10) was purchased from Vectashield (USA). Pierce BCA Protein Assay Kit, Pierce Co-Immunoprecipitation Kit, and Halt Protease and Phosphatase Inhibitor Cocktail were from Thermo Fisher Scientific (USA). The purified fusion peptides, active Tat–PSD-95 wild-type PDZ2 peptide (referred to as PSD-95 wild-type PDZ2 peptides and wild-type PDZ2 peptide), and inactive Tat–PSD-95 mutant PDZ2 peptide (referred to as PSD-95 mutant PDZ2 peptide and mutant PDZ2 peptide in this manuscript) were purchased from Creative BioMart (USA) and used as previously described.[19] 10× Tris-buffered saline (1706435), 4× Laemmli sample buffer, 4 to 15% Criterio TG Precast Midi Protein Gels, and 10× Tris/glycine/sodium dodecyl sulfate buffer (1610732) were purchased from Bio-Rad (USA).

Animals

This study was implemented with approval from the Animal Care and Use Committee at Johns Hopkins University (Baltimore, Maryland) and was consistent with the Guide for the Care and Use of Laboratory Animals from the National Institutes of Health (Bethesda, Maryland). Wild-type C57BL/6 mice of both sexes (The Jackson Laboratory, USA) were maintained on a 12:12 h light:dark cycle, on corncob bedding (7097 Teklad, Envigo, USA), with *ad libitum* access to chlorinated reverse-osmosis water and rodent diet (2018sx Teklad global 18% protein, Envigo, USA), and environmental enrichment in the form of Nestlets (Ancare, USA). Water and food were available *ad libitum* until mice were transported to the laboratory approximately 1 h before the experiments. For *in vivo* experiments, postnatal day 7 mice were randomly assigned to control and treatment groups. For *in vitro* experiments, postnatal day 0 to 1 litters were collected for preparation of primary neuronal cultures.

In Vivo Model of Anesthetic Neurotoxicity

Neonatal mice at postnatal day 7 were exposed to 1.5% isoflurane in 50% O_2 for 4 h at a flow rate of 3 l/min, with airflow as the carrier (isoflurane group). Control animals were exposed to 50% O_2 (oxygen control group). All the mice were placed in a clear plastic cones and body temperature maintained by a heating pad set to 37°C. The purified fusion peptides, active PSD-95 wild-type PDZ2 peptide, or inactive PSD-95 mutant PDZ2 peptide at 8 mg/kg were injected into mice at postnatal day 7 intraperitoneally in 150 μl of phosphate-buffered saline and 10% glycerol, as previously described.[19] Four hours after gas exposures or peptide injections, mice were decapitated, and hippocampal regions were dissected from the brain. The hippocampal tissue was pooled from two mice in every group for each independent experiment to attain sufficient protein for coimmunoprecipitation. For the behavior experiments, mice at postnatal day 7 were randomly assigned to four groups: (1) oxygen control + vehicle, (2) oxygen control + YC-1, (3) isoflurane + vehicle, and (4) isoflurane + YC-1. Mice in the oxygen control + YC-1 and isoflurane + YC-1 groups received 2 mg/kg of intraperitoneal injections of YC-1 at the time of isoflurane exposure. The mice in the oxygen control + vehicle and isoflurane + vehicle groups received 1% dimethyl sulfoxide. The solution of YC-1 was prepared in 1% dimethyl sulfoxide and was injected in the cohorts as previously described.[26,27]

Primary Neuronal Culture

Brain hippocampi were microdissected from postnatal day 0 to 1 pups. Then blood vessels and meninges were removed in ice-cold dissecting solution (1× Hank's Balanced Salt solution, 1× penicillin/streptomycin, 1 mM sodium pyruvate, 10 mM N-2-hydroxyethylpiperazine-N-2-ethane sulfonic acid, and 30 mM glucose). The brain tissue was chopped into smaller pieces and digested using the Papain Dissociation kit according to the manufacturer's instructions (Worthington, USA). Gently minced hippocampal tissue was incubated with Papain-deoxyribonuclease solution (20 U/ml papain and 0.005% deoxyribonuclease) for 30 min at 37°C with slow agitation. The suspension was triturated with a sterile fire-polished glass pipette and then centrifuged at 4°C for 5 min at 300*g*. The pellet was resuspended in Earle's Balanced Salt Solution containing ovomucoid protease inhibitor with bovine serum albumin and deoxyribonuclease. Next, a discontinuous density gradient was prepared by pipetting the cell suspension onto a 5-ml layer of albumin-ovomucoid inhibitor solution. The gradient was centrifuged at 70*g* for 6 min at room temperature. The supernatant containing noncellular debris was discarded, and the cell pellet was resuspended in neurobasal medium supplemented with 1× GlutaMAX, 2% B27, 1% penicillin–streptomycin, and 1% heat-inactivated horse serum. Cells were seeded on poly-D-lysine– and laminin-coated glass chamber slides at a plating density of around 2.5 to 3.5×10^4 cells per well and grown in a humidified carbon dioxide incubator at 37°C. Cytosine arabinoside (2 μM) was added to the cultures on the third day after plating to inhibit the proliferation of glial cells. Half of the culture medium was changed every alternate day. The purity of the primary neuronal cells was assessed with neuronal marker MAP-2.

In Vitro Model of Anesthetic Neurotoxicity

At 7 days *in vitro*, neuronal cells were placed in humidified airtight gas chambers and exposed to 1.5% isoflurane in a gas of 25% O_2 and 5% CO_2 that was balanced with N_2. Control neurons were exposed only to carrier gas. The gas chambers were carefully monitored with a digital gas monitor. The chambers were placed in a standard 37°C incubator for 4 h. Neuronal cells were treated with pharmacologic inhibitors and activators to delineate the downstream signaling mechanisms in response to isoflurane or synaptic PSD-95 PDZ2 domain disruption.

Cell Viability Assay

Neuronal cell viability was measured with the 3-(4,5-dimethylthiazol-2-yl)-2,5-diphenyltetrazolium bromide assay according to the manufacturer's protocol (ab211091, Abcam, United Kingdom). Briefly, we seeded hippocampal neuronal cells around 1 to 2×10^4 cells/well in triplicate onto Poly-D-Lysine-laminin–coated 96-well plates. At 7 days *in vitro*, cells were exposed and treated for 4 h with vehicle gas and 1.5% isoflurane or 1 μM inactive PSD-95 mutant PDZ2 peptide and 1 μM active PSD-95 wild-type PDZ2 peptide. Absorbance was measured at 590 nm on the Spark Multimode microplate reader (Tecan, Switzerland) to determine neuronal cell viability. Wells containing only media were used for blank absorbance reading. The cell viability was expressed as a percentage normalized relative to the viability in untreated cells.

Immunocytochemistry

Primary neuronal cells were fixed in 4% paraformaldehyde solution for 10 to 15 min, washed in phosphate-buffered saline three times (5-min intervals), and then blocked with blocking solution (2% normal goat serum + 1% bovine serum albumin + 0.1% Tween-20) in phosphate-buffered saline for 45 min at room temperature. Then cells were incubated with primary antibodies to MAP-2, (anti-chicken, 1:500), drebrin (anti-rabbit, 1:250), synaptophysin (anti-rabbit, 1:500), and PSD-95 (anti-mouse, 1:500) in blocking solution overnight at 4°C. Cells were washed three times in phosphate-buffered saline (5-min intervals) and incubated with Alexa Fluor–conjugated secondary antibody cocktails in phosphate-buffered saline containing 0.2% bovine serum albumin for 2 h at room temperature. After incubation, cells were washed five times in phosphate-buffered saline to remove excess secondary antibody and then mounted with ProLong diamond mounting medium. Images were captured using a LSM880-Airyscan fast super-resolution laser scanning confocal microscope (Zeiss, Jena, Germany) and Leica SPE DMI8 (USA).

Dendritic Spine Analysis

Primary hippocampal neurons were fixed and coimmunostained with drebrin and MAP-2 antibodies. Images were taken using Zeiss LSM880-Airyscan fast superresolution laser scanning confocal microscope. All images were taken using Plan-Apochromat 63×/1.4 oil differential interference contrast. The image size scaling (per pixel) is around 0.06 μm × 0.06 μm × 0.19 μm. We analyzed drebrin-positive dendritic spines using Imaris software (Bitplane, Oxford Instruments, Bognor Regis, UK). Spines that emanated directly from the MAP-2–positive dendritic shaft were analyzed, and spines whose structure was not completely visible were excluded. For each neuron, spines along secondary or tertiary dendrites were imaged and selected for spine density quantification. Dendritic branches were reconstructed by using Imaris and were analyzed for spine density and length. Spine densities were calculated by quantifying the number of spines per 10 μm length of dendrite. Four to five independent cultures were performed per experimental condition (*i.e.*, per group). In total, 25 to 40 neurons were analyzed per experimental condition for spine analysis. The results are expressed as mean spine density per 10 μm dendrite length. Blinding was performed such that all the groups were labeled differently at the time of imaging and analysis.

Coimmunoprecipitation and Western Blotting

Mice were euthanized by decapitation, and hippocampal regions were dissected from the brain under a dissecting microscope. Total protein was extracted and subjected to coimmunoprecipitation with the Pierce Co-Immunoprecipitation Kit (Thermo Scientific, USA) according to the manufacturer's instructions. In brief, the hippocampal tissue was dissected and homogenized in a bead homogenizer in the presence of ice-cold Radio-Immunoprecipitation Assay buffer (0.025 M Tris, 0.15 M NaCl, 0.001 M EDTA, 1% NP-40, 5% glycerol, pH 7.4) supplemented with a protease and phosphatase inhibitor cocktail. The crude homogenates were centrifuged at 16,000*g* for 20 min at 4°C. The lysates were collected, and the protein concentration estimated with the Pierce BCA Protein Assay Kit (Thermo Fisher Scientific, USA), according to the manufacturer's instructions. The protein lysates were precleaned in a column of agarose resin that was incubated at 4°C for 45 min with gentle end-over-end mixing. Next, the column was centrifuged at 1,000*g* for 1 min. The flow-through containing the cleaned protein lysate was collected and the column discarded. Equal amounts of protein were incubated with 5 μg of affinity-purified rabbit-NMDA-R2A&B antibody for 4 h and then immunoprecipitated with protein A/G agarose beads. Beads were washed three times with lysis buffer for 1 min each before immunoprecipitation. The protein was then resolved by sodium dodecyl sulfate-polyacrylamide gel electrophoresis and immunoblotted through Western blotting. Briefly, proteins from the gel were transferred to polyvinylidene difluoride membranes (Millipore, USA). The membranes were blocked in Tris-buffered saline + 0.1% Tween-20 containing 5% nonfat milk for 1 h at room temperature, and then incubated with primary antibodies to PSD-95 (1:1,000) or NMDAR2A&B (1:1,000) in Tris-buffered saline + 0.1% Tween-20 containing 5% nonfat milk overnight at 4°C. Membranes were washed three times for 10 min each in Tris-buffered saline + 0.1% Tween-20 and then incubated for 2 h with horseradish peroxidase–conjugated anti-rabbit or anti-mouse immunoglobulin at a dilution of 1:5,000. Finally, the membranes were washed to remove excess secondary antibody. Proteins were visualized with enhanced chemiluminescence (Amersham, USA) and images captured with the ChemiDoc Imaging System (Bio-Rad, USA). PSD-95 coimmunoprecipitate was quantified relative to NMDAR2A&B precipitate using Bio-Rad Quantity One image analysis software.

Measurement of cGMP-dependent Protein Kinase Activity

cGMP-dependent protein kinase activity was determined with the CycLex assay kit (MBL International, USA) according to the manufacturer's protocol. Briefly, primary hippocampal neurons were plated in six-well plates at 1.5 to 2×10^6 cells per well and treated with gases or peptides along with pharmacologic activators and inhibitors. Then the neuronal cells were lysed with freeze-thaw cycles before being centrifuged for 20 min at 14,000*g*. Finally, the lysates were added to wells coated with recombinant G-kinase substrates. The absorbance was measured from 450 nm to 550 nm on the Spark Multimode microplate reader.

Synaptic Puncta Quantification

Synapse quantification was performed using custom-written plugin Puncta Analyzer for quantification of colocalized synaptic puncta as described in a study published by Ippolito and Eroglu.[28] Briefly, primary neuronal cells were fixed in 4% paraformaldehyde and coimmunostained for presynaptic marker synaptophysin, postsynaptic marker PSD-95, and neuronal marker MAP-2. Confocal images were taken using Zeiss LSM880-Airyscan fast super-resolution laser scanning confocal microscope. All images were taken using Plan-Apochromat 63×/1.4 Oil differential interference contrast with scaling x = 0.043 μm and y = 0.043 μm. The image size was x, 73.9 μm, and y, 73.9 μm in single plane. MAP-2–positive neurons with soma and dendrites were centered in the field of view and were imaged. Synapses were quantified by analyzing colocalization of synaptophysin and PSD-95 puncta using a plugin puncta analyzer in ImageJ (National Institutes of Health, USA). The background of all the images was removed separately from the red and green channel using the rolling ball radius of 50. Next, thresholding was performed for detecting discrete puncta, and puncta were identified in red and green channels using the Puncta Analyzer plugin. Colocalized puncta were counted as a synapse.[28] Four independent cultures were performed per experimental condition (*i.e.*, per group). In total, 30 to 40 neurons were analyzed per experimental condition for synapse quantification. For each independent culture, similar regions of interest including soma and all the dendritic fragments of neurons were assessed for colocalization as previously described.[29]

Novel Object Recognition

The novel object recognition procedure was performed as reported in our previous studies[17,18] and was used to evaluate nonspatial hippocampal memory.[30,31] Briefly, it was composed of two sessions, a familiarization session during which mice were allowed to freely explore two similar objects within an opaque box (40 cm width × 40 cm length × 34 cm height) for 10 min, followed by a second session after 2 h, which was a test session, in which one of the objects was replaced by a novel or unacquainted object. Mice innately prefer to explore the novel object rather than the familiar one, and a preference for the novel object demonstrates intact memory for the familiar object. After 2 h, the object recognition was tested, where a novel object was substituted for one of the familiar training objects and then mice were allowed to explore for 5 min. Object investigation time was determined by the amount of time the mouse spent in the zone immediately surrounding the object. Only mice that investigated any object for at least 10 s (criterion) were taken into consideration. During the testing phase, mice (n = 8) did not meet the criterion and so were not included in the analysis. Data were recorded with a video camera, and time spent with each object was analyzed by ANYmaze software (Stoelting, USA).

Statistical Analysis

All data were tested for normality using the Shapiro–Wilk test and then presented as mean ± SD. The paired or independent unpaired two-tailed Student's t test or one-way ANOVA was used for statistical analysis. For multiple testing corrections, the Tukey *post hoc* test was used when data were compared between all the groups. The Bonferroni *post hoc* test was used when data between selected groups were compared; coimmunoprecipitation analysis (comparing control, isoflurane, and PSD-95 mutant PDZ2 peptide, PSD-95 wild-type PDZ2 peptide, which included one family, four treatments, and two comparisons), total spine density, and relative cGMP-dependent protein kinase activity (comparing control, isoflurane, control + DETA NONOate, control + DETA NONOate + ODQ, isoflurane + DETA NONOate, isoflurane + DETA NONOate + ODQ, which included one family, six treatments, and four comparisons) and (PSD-95 mutant PDZ2 peptide, PSD-95 wild-type PDZ2 peptide, PSD-95 mutant PDZ2 peptide + DETA NONOate, PSD-95 mutant PDZ2 peptide + DETA NONOate + ODQ, PSD-95 wild-type PDZ2 peptide + DETA NONOate, PSD-95 wild-type PDZ2 peptide + DETA NONOate + ODQ, which included one family, six treatments, and four comparisons), (comparing control, isoflurane, control + 8-Br–cGMP, control + 8-Br–cGMP + KT5823, isoflurane + 8-Br–cGMP, isoflurane + 8-Br–cGMP + KT5823, which included one family, six treatments, and four comparisons) and (comparing PSD-95 mutant PDZ2 peptide, PSD-95 wild-type PDZ2 peptide, PSD-95 mutant PDZ2 peptide + 8-Br–cGMP, PSD-95 mutant PDZ2 peptide + 8-Br–cGMP + KT5823, PSD-95 wild-type PDZ2 peptide + 8-Br–cGMP, PSD-95 wild-type PDZ2 peptide + 8-Br–cGMP + KT5823, which included one family, six treatments, and four comparisons); for synapse puncta quantification (comparing control, isoflurane, control + 8-Br–cGMP, control + 8-Br–cGMP + KT5823, isoflurane + 8-Br–cGMP, isoflurane + 8-Br–cGMP + KT5823, control + YC-1, isoflurane + YC-1, which included one family, eight treatments, and five comparisons) and (comparing PSD-95 mutant PDZ2 peptide, PSD-95 wild-type PDZ2 peptide,

PSD-95 mutant PDZ2 peptide + 8-Br–cGMP, PSD-95 mutant PDZ2 peptide + 8-Br–cGMP + KT5823, PSD-95 wild-type PDZ2 peptide + 8-Br–cGMP, PSD-95 wild-type PDZ2 peptide + 8-Br–cGMP + KT5823, PSD-95 mutant PDZ2 peptide + YC-1, PSD-95 wild-type PDZ2 peptide + YC-1, which included one family, eight treatments and five comparisons). Sample sizes were chosen based on preliminary data and/or published studies. A sample size of $n = 3$ was chosen for coimmunoprecipitation experiment because $n = 3$ was sufficient to show the disruption of interactions between NMDAR NR2 subunits and PSD-95 in response to cell-permeant fusion peptide.[19] A sample size of $n = 4$ to 5 independent culture experiments in which a total of 25 to 40 neurons were analyzed per experimental conditions for spine analysis was chosen because $n = 3$ to 6 experiments in which 30 dendritic segments in total were sufficient to show significant differences in spines density in primary neuronal cultures.[29,32] A sample size of $n = 4$ independent culture experiments in which a total of 30 to 40 neurons were analyzed per experimental condition was chosen for synapse quantification because around 30 neurons were sufficient to show significant differences in synapse density.[33] A sample size of $n = 3$ was chosen for studying the cGMP-dependent protein kinase activity because $n = 3$ was sufficient to show the effects of icariside II against oxygen glucose deprivation–induced primary hippocampal neuron injury to enhance cGMP level and PKG activity.[34] All the n numbers (n = number of independent culture or experiments) are reported in the figure legends. In the novel object recognition test, male and female data were separated and analyzed in a one-way ANOVA followed by Bonferroni *post hoc* test (comparing oxygen control + vehicle, oxygen control + YC-1, isoflurane + vehicle, and isoflurane + YC-1, which included one family, four treatments, and three comparisons). Because all animals survived, there were no missing data in this study. Outlier value was detected by GraphPad Prism (robust regression and outlier removal Q = 1%), so it was removed. Using means and SD of recognition index from mixed sex control and isoflurane group, we determined the sample size needed for 90% power and $\alpha = 0.05$ was $n = 9$ mice. Thus, power is greater than 90% with males ($n = 15$; Cohen's $d = 1.29$) and females ($n = 14$; Cohen's $d = 1.45$). Statistical significance was set at $P < 0.05$. All statistical analyses were carried out with GraphPad Prism version 8.4.3 (GraphPad Inc., USA).

Results

Isoflurane or PSD-95 Wild-type PDZ2 Peptide Disrupt PDZ2 Domain–mediated Protein Interactions between NMDAR NR2A/2B and PSD-95 in the Mouse Hippocampus

To examine whether isoflurane exposure disrupts synaptic PDZ2 domain–mediated protein interactions in the developing brain hippocampus, we exposed postnatal day 7 mouse pups to isoflurane or control conditions (50% oxygen) for 4 h. A separate cohort was administered intraperitoneal injection of fusion peptides, active PSD-95 wild-type PDZ2 peptide (mimics isoflurane), or inactive PSD-95 mutant PDZ2 peptide (an inactive control). Under normal conditions, the second PDZ domain of PSD-95 interacts with the PDZ domain of nNOS or the C-terminal tails of the NR2A and NR2B subunits.[16] Through the coimmunoprecipitation assay, we found that isoflurane and PSD-95 wild-type PDZ2 peptide markedly disrupted the interactions between NR2A/2B subunits and PSD-95 in the hippocampal lysates. However, in control and PSD-95 mutant PDZ2 peptide groups, this interaction was retained (fig. 1, A and B). Data were analyzed by using one-way ANOVA, which showed that the levels of PSD-95 coimmunoprecipitate relative to NR2A/2B precipitate (mean ± SD [in percentage of control]) were decreased in isoflurane (54.73 ± 16.52) compared with control, $P = 0.001$; and in PSD-95 wild-type PDZ2 peptide (51.32 ± 12.93) compared with PSD-95 mutant PDZ2 peptide, $P = 0.001$ ($n = 3$).

Exposure of Isoflurane or PSD-95 Wild-type PDZ2 Peptide on Cell Viability and Dendritic Spine Density in Primary Hippocampal Neurons

The purity of primary neuronal cells was assessed with MAP-2/4′,6-diamidino-2-phenylindole immunostaining, and in total, 85% of the cells were positive for MAP-2 proteins (fig. 2A). At 7 days, *in vitro* cells were exposed and treated for 4 h, and 3-(4,5-dimethylthiazol-2-yl)-2,5-diphenyltetrazolium bromide assay showed that neither 1.5% isoflurane nor 1 μM active PSD-95 wild-type PDZ2 peptide reduced viability in the hippocampal neurons when compared to that of respective control or untreated neurons (fig. 2, B and C). Data were analyzed using one-way ANOVA, which showed no significant differences in cell viability (in percentage) between untreated and experimental groups ($n = 3$ independent culture experiments). The results were as follows: untreated *versus* control, $P = 0.909$; untreated *versus* isoflurane, $P = 0.783$; control (94.53 ± 24.93) *versus* isoflurane (91.12 ± 12.18), $P = 0.963$; untreated *versus* PSD-95 mutant PDZ2 peptide, $P = 0.994$; untreated *versus* PSD-95 wild-type PDZ2 peptide, $P = 0.960$; and PSD-95 mutant PDZ2 peptide (99.1 ± 9.97) *versus* PSD-95 wild-type PDZ2 peptide (97.49 ± 16.76), $P = 0.983$. PSD-95 is a fundamental scaffolding protein during synaptogenesis and neurodevelopment, and its dysfunction during development may alter synaptic plastic events at the dendritic spines, causing neurologic deficits.[35] Therefore, we examined whether isoflurane or loss of synaptic PDS95-PDZ2 and NR2A/2B protein interaction affects early dendritic spines in developing hippocampal neuronal cells. After exposure to 4 h of 1.5% isoflurane or 1 μM active PSD-95 wild-type PDZ2 peptide, neurons exhibited significant spine loss in comparison with their respective controls

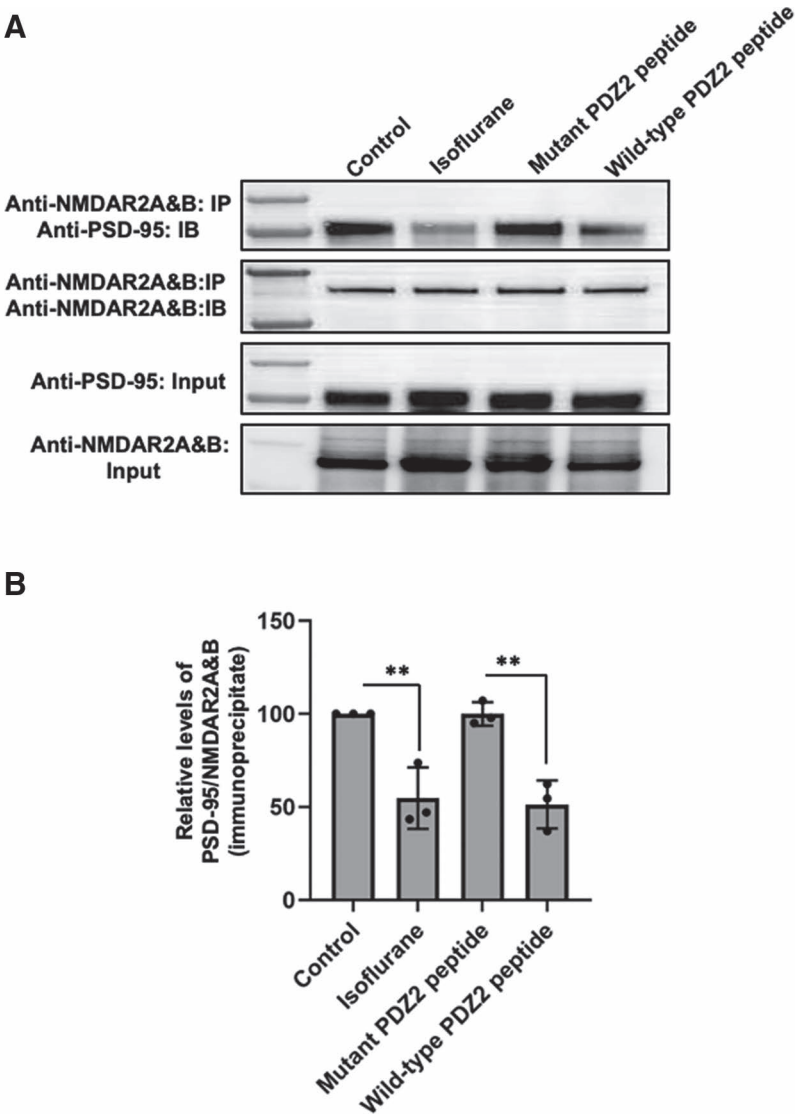

Fig. 1. Disruption of *N*-methyl-d-aspartate receptor (NMDAR) NR2A/2B and postsynaptic density (PSD)-95–PDZ2 protein interactions by isoflurane and PSD-95 wild-type PDZ2 peptide in the hippocampus of neonatal mouse brain. At postnatal day 7, mouse brains were harvested immediately after exposure to control conditions (50% oxygen: control), 1.5% isoflurane in 50% O_2 (isoflurane), 8 mg/kg inactive PSD-95 mutant PDZ2 peptide (referred to as mutant PDZ2 peptide) or 8 mg/kg active PSD-95 wild-type PDZ2 peptide (referred to as wild-type PDZ2 peptide). (*A*) Representative Western blot shows coimmunoprecipitation of PSD-95 and NMDAR2A&B subunits in control, isoflurane, PSD-95 mutant PDZ2 peptide, and PSD-95 wild-type PDZ2 peptide–treated groups. Represented are equal amounts of the NMDAR2A&B immunoprecipitated from mouse brain hippocampus with NMDAR2A&B antibody. The amount of sample loaded for the input was 10% of that for the immunoprecipitation. (*B*) Representative densitometric analysis of PSD-95 coimmunoprecipitate relative to NMDAR2A&B precipitate. Data represent mean ± SD; $n = 3$ independent experiments. $^{**}P < 0.01$ compared to respective control. Data were analyzed using one-way ANOVA with Bonferroni multiple comparisons test.

(mean ± SD [spine density per 10 μm]) as follows: control (5.28 ± 0.56) *versus* isoflurane (2.23 ± 0.67), $P<0.0001$; PSD-95 mutant PDZ2 peptide (4.74 ± 0.94) *versus* PSD-95 wild-type PDZ2 peptide (1.47 ± 0.87), $P<0.001$; fig. 2, D to G). Additionally, we observed a significant increase in spine length in response to PSD-95 wild-type PDZ2 peptide exposure (PSD-95 mutant PDZ2 peptide [1.36 ± 0.39] *versus* PSD-95 wild-type PDZ2 peptide [2.28 ± 0.48], $P = 0.011$) and a trend toward increased spine length in response to isoflurane exposure (control [1.48 ± 0.25] *versus* isoflurane [1.99 ± 0.49], $P = 0.076$), although the latter change was not statistically significant (fig. 2, H and I). Data were analyzed by using independent two-tailed unpaired *t*-test.

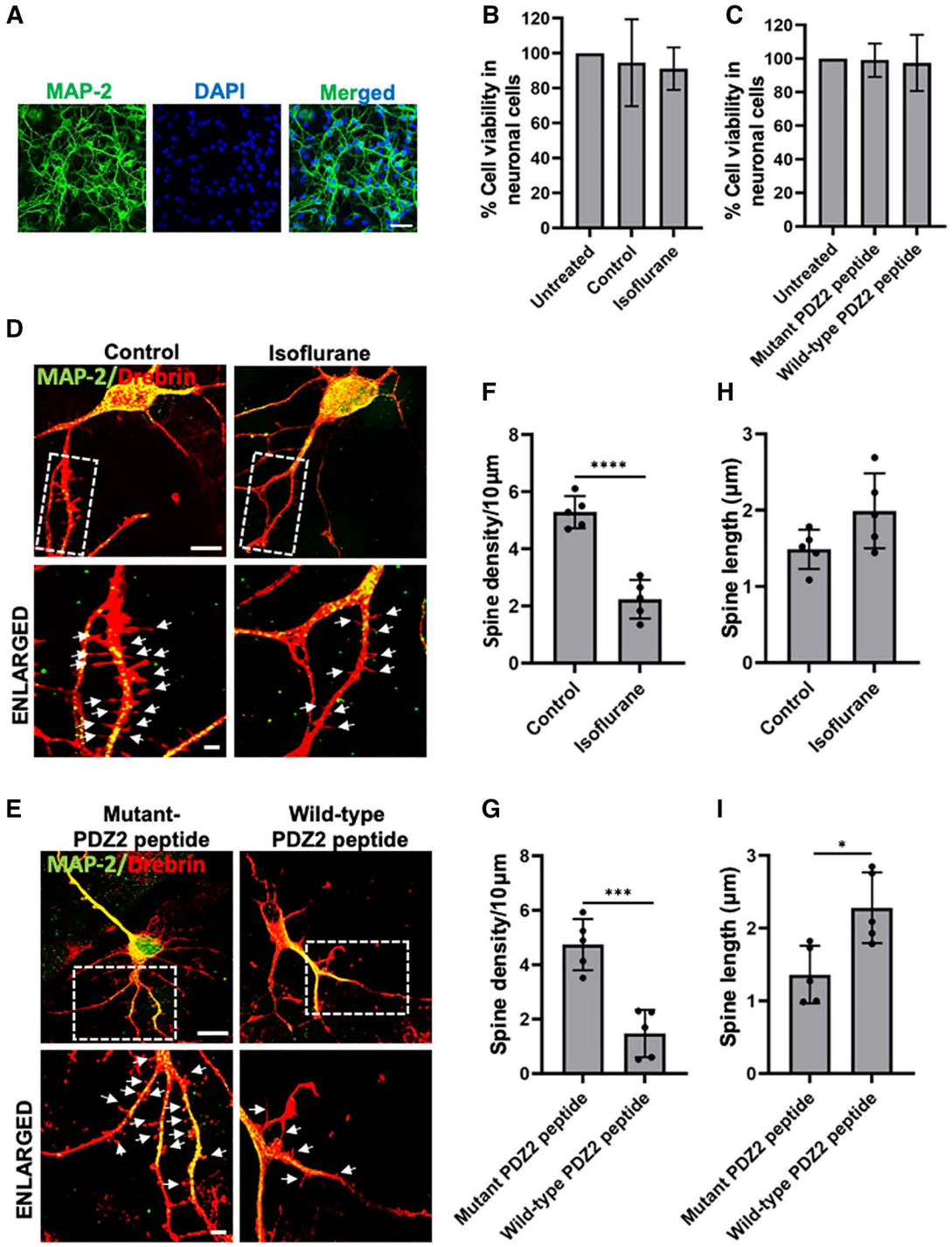

Fig. 2. Effect of isoflurane and postsynaptic density (PSD)-95 wild-type PDZ2 peptide on neuronal cell viability and dendritic spines. Primary hippocampal neurons were cultured until 7 days *in vitro*. (*A*) Representative fluorescent photomicrograph (40×) with neuronal-specific marker microtubule-associated protein-2 (MAP-2). 4′,6-diamidino-2-phenylindole counterstain was used to identify nuclei. *Scale bar* = 5 µm. (*B* and *C*) Neuronal cells were exposed for 4 h to control conditions of 25% O_2 and 5% CO_2 that was balanced with N_2 or to 1.5% isoflurane in a gas of 25% O_2 and 5% CO_2 that was balanced with N_2. Other hippocampal neurons were exposed to 1 µM inactive PSD-95 mutant PDZ2 peptide or 1 µM active PSD-95 wild-type PDZ2 peptide for 4 h. Cell viability was assessed with the 3-(4,5-dimethylthiazol-2-yl)-2,5-diphenyltetrazolium bromide assay. Viability was not significantly different in the experimental, control, and untreated groups. Data represent mean ± SD, $n = 3$ independent culture experiments, and were analyzed by one-way ANOVA with Tukey multiple comparisons test. (*D* and *E*) Neuronal cells

NO-mediated Activation of sGC Prevents Isoflurane- and PSD-95 Wild-type PDZ2 Peptide–induced Loss in Early Dendritic Spines in Primary Hippocampal Neurons

NO signaling plays an important role in regulating the development of excitatory synapses, and impairment in NO production interferes with the development of spines and synapses.[36] We investigated the effects of the NO donor DETA NONOate on isoflurane- and PSD-95 wild-type PDZ2 peptide–induced loss of early dendritic spines in hippocampal neurons. First, we determine the noncytotoxic concentration of DETA NONOate and sGC inhibitor ODQ in neuronal cells (data not shown). Addition of 150 μM DETA NONOate at the time of isoflurane or PSD-95 wild-type PDZ2 peptide exposure attenuated the loss of dendritic spines in neuronal cells (mean ± SD [spine density per 10 μm]). Data were analyzed using one-way ANOVA, and total spine density was measured in response to DETA NONOate and ODQ in isoflurane- and PSD-95 wild-type PDZ2 peptide–treated neuronal cells as follows: isoflurane (1.82 ± 0.83) *versus* isoflurane + DETA NONOate (3.25 ± 0.31), $P = 0.037$; PSD-95 wild-type PDZ2 peptide (1.69 ± 0.73) *versus* PSD-95 wild-type PDZ2 peptide + DETA NONOate (3.14 ± 0.5), $P = 0.030$; (fig. 3, A to D). To determine whether activation of sGC by NO is specific and sufficient to prevent isoflurane- and PSD-95 wild-type PDZ2 peptide–induced loss in spine density, we treated neuronal cells with ODQ (100 μM) along with DETA NONOate. ODQ blocked the ability of DETA NONOate to attenuate isoflurane and PSD-95 wild-type PDZ2 peptide–induced dendritic spine loss as follows: isoflurane + DETA NONOate *versus* isoflurane + DETA NONOate + ODQ (1.21 ± 0.2), $P = 0.002$; isoflurane *versus* isoflurane + DETA NONOate + ODQ, $P = 0.903$; PSD-95 wild-type PDZ2 peptide + DETA NONOate *versus* PSD-95 wild-type PDZ2 peptide + DETA NONOate + ODQ (1.13 ± 0.17), $P = 0.002$; and PSD-95 wild-type PDZ2 peptide *versus* PSD-95 wild-type PDZ2 peptide + DETA NONOate + ODQ, $P > 0.999$; (fig. 3, A to D).

Fig. 2. (*Continued*). were coimmunostained with MAP-2 and drebrin. Representative confocal photomicrographs (63×) show dendritic segments and spines after isoflurane (*D*) or PSD-95 wild-type PDZ2 peptide (*E*) exposures. *Bottom*, 2× zoom image of the boxed areas at the *top*. *Arrows* indicate the dendritic spines. *Scale bar* = 20 μm *top* and 5 = μm *bottom*. (*F* and *G*) Summary plots represent total spine density per 10 μm dendrite length after isoflurane (*F*) or PSD-95 wild-type PDZ2 peptide (*G*) exposure in comparison with respective controls. (*H* and *I*) Summary plots represent mean spine length after isoflurane (*H*) or PSD-95 wild-type PDZ2 peptide (*I*) exposure in comparison with respective controls. PSD-95 mutant PDZ2 peptide (referred to as mutant PDZ2 peptide) and PSD-95 wild-type PDZ2 peptide (as wild-type PDZ2 peptide). Data were analyzed by independent two-tailed unpaired *t*-test. Data represent mean ± SD; n = 5 independent experiments for spine density and spine length. *$P < 0.05$, ***$P < 0.001$, ****$P < 0.0001$ compared with respective control.

8-Br–cGMP—mediated Activation of PKG Prevents Isoflurane- and PSD-95 Wild-type PDZ2 Peptide–induced Loss in Dendritic Spines and Decline in the cGMP-dependent Protein Kinase Activity in Hippocampal Neurons

Multiple effects of NO are mediated through its canonical receptor, sGC, and the secondary messenger cGMP.[37] Therefore, we investigated the effects of the cGMP analog 8-Br–cGMP on isoflurane- and PSD-95 wild-type PDZ2 peptide–induced dendritic spine loss. First we determined the noncytotoxic concentration of 8-Br–cGMP and PKG inhibitor KT5823 in neuronal cells (data not shown). The addition of 200 μM 8-Br–cGMP at the time of isoflurane or PSD-95 wild-type PDZ2 peptide exposure attenuated the loss of dendritic spines in the hippocampal neuronal cells (mean ± SD [spine density per 10 μm]). Data were analyzed using one-way ANOVA, and spine density were measured in response to 8-Br–cGMP and KT5823 in isoflurane- and PSD-95 wild-type PDZ2 peptide–treated cells. Isoflurane (1.69 ± 0.49) *versus* isoflurane + 8-Br–cGMP (3.52 ± 0.8), $P = 0.045$, (fig. 4, A and C). 8-Br–cGMP also attenuated PSD-95 wild-type PDZ2 peptide–induced loss of spine density, as follows: PSD-95 wild-type PDZ2 peptide (1.52 ± 0.61) *versus* PSD-95 wild-type PDZ2 peptide + 8-Br–cGMP (3 ± 0.42), $P = 0.048$, (fig. 4, B and D). Next, to determine whether activation of PKG by 8-Br–cGMP is specific and sufficient to prevent isoflurane and PSD-95 wild-type PDZ2 peptide–induced loss in spine density, we added 1 μM KT5823 along with 8-Br–cGMP. We found that KT5823 blocked the ability of 8-Br–cGMP to prevent isoflurane-induced spine loss, as follows: isoflurane + 8-Br–cGMP *versus* isoflurane + 8-Br–cGMP + KT5823 (1.66 ± 0.43), $P = 0.041$; isoflurane *versus* isoflurane + 8-Br–cGMP + KT5823, $P > 0.999$, (fig. 4, A and C); and PSD-95 wild-type PDZ2 peptide–induced spine loss as follows: PSD-95 wild-type PDZ2 peptide + 8-Br–cGMP *versus* PSD-95 wild-type PDZ2 peptide + 8-Br–cGMP + KT5823 (1.49 ± 0.56), $P = 0.042$; PSD-95 wild-type PDZ2 peptide *versus* PSD-95 wild-type PDZ2 peptide + 8-Br–cGMP+KT5823, $P > 0.999$, (fig. 4, B and D), indicating that this pathway is PKG-dependent. cGMP-dependent protein kinase is involved in long-term potentiation and in synaptic plasticity,[38] and cGMP-dependent protein kinase type I is detectable in dissociated cultures of hippocampal neurons.[39] To determine changes in cGMP-dependent protein kinase activity in response to isoflurane or synaptic PDZ2 disruption, we exposed hippocampal neurons to isoflurane or PSD-95 wild-type PDZ2 peptide in the presence/absence of 8-Br–cGMP and KT5823. Both isoflurane and PSD-95 wild-type PDZ2 peptide caused a decrease in cGMP-dependent protein kinase activity. Data were analyzed by one-way ANOVA to compare relative

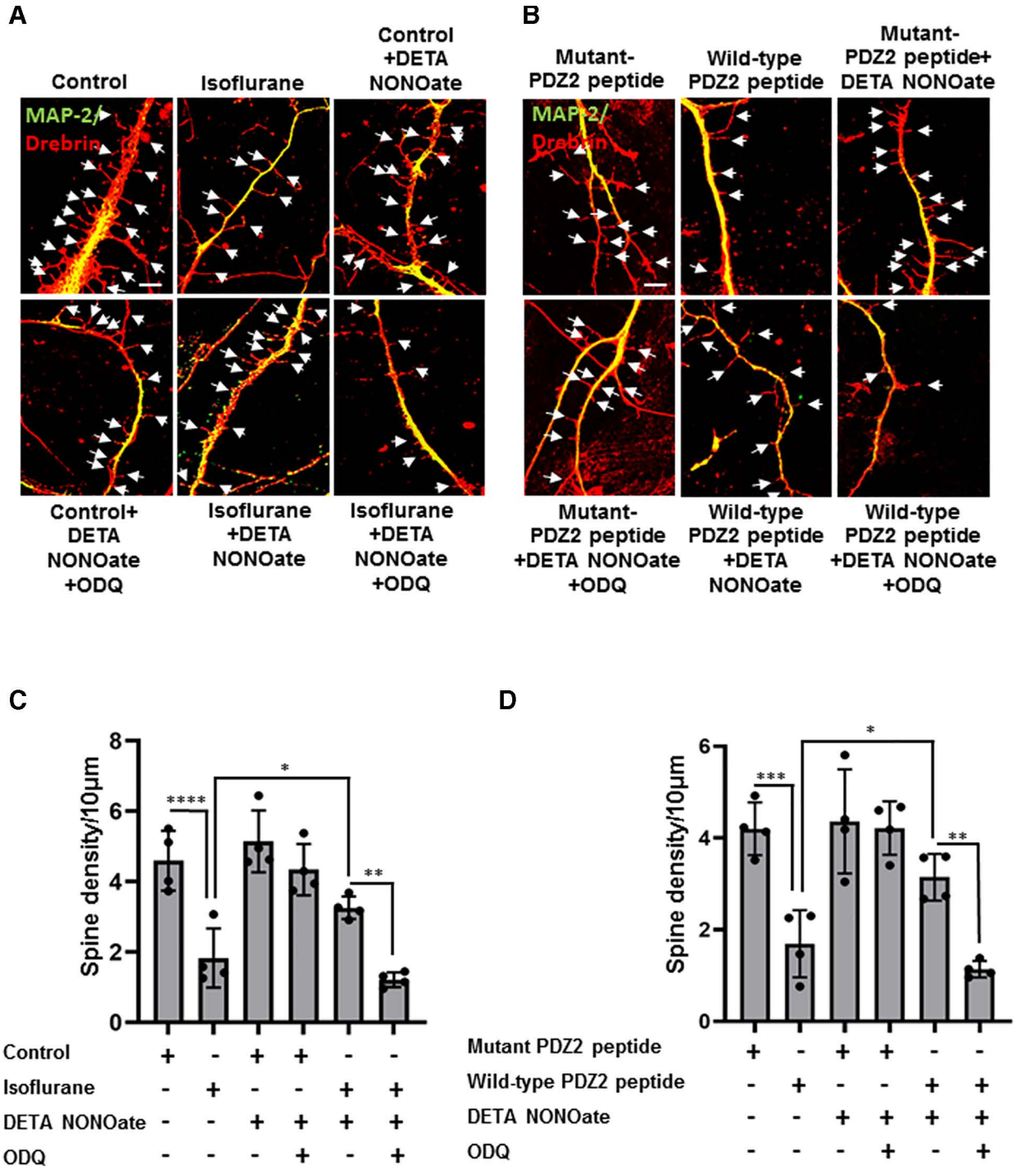

Fig. 3. Soluble guanylate cyclase inhibitor 1H-[1,2,4] oxadiazolo[4,3-a]quinoxalin-1-1 (ODQ) blocked the ability of NO donor DETA NONOate to prevent isoflurane and postsynaptic density (PSD)-95 wild-type PDZ2 peptide–induced dendritic spine loss. (*A* and *B*) Primary neuronal cells were pretreated with the DETA NONOate or the soluble guanylyl cyclase (sGC) inhibitor ODQ for 4 h, neuronal cells were exposed to the conditions shown and were coimmunostained for microtubule-associated protein-2 (MAP-2)/drebrin, and total spine density was calculated. Representative photomicrographs (63×) show dendritic spines in the hippocampal neurons after respective treatments; *scale bar* = 10 µm. *Arrows* indicate the dendritic spines. (*C* and *D*) Summary plots represent spine density per 10 µm dendrite length. PSD-95 mutant PDZ2 peptide (referred to as mutant PDZ2 peptide) and PSD-95 wild-type PDZ2 peptide (as wild-type PDZ2 peptide). Data were analyzed using one-way ANOVA with Bonferroni multiple comparisons test. Data represent mean ± SD; $n = 4$ independent experiments. *$P < 0.05$, **$P < 0.01$, ***$P < 0.001$, ****$P < 0.0001$ compared to respective control or as indicated.

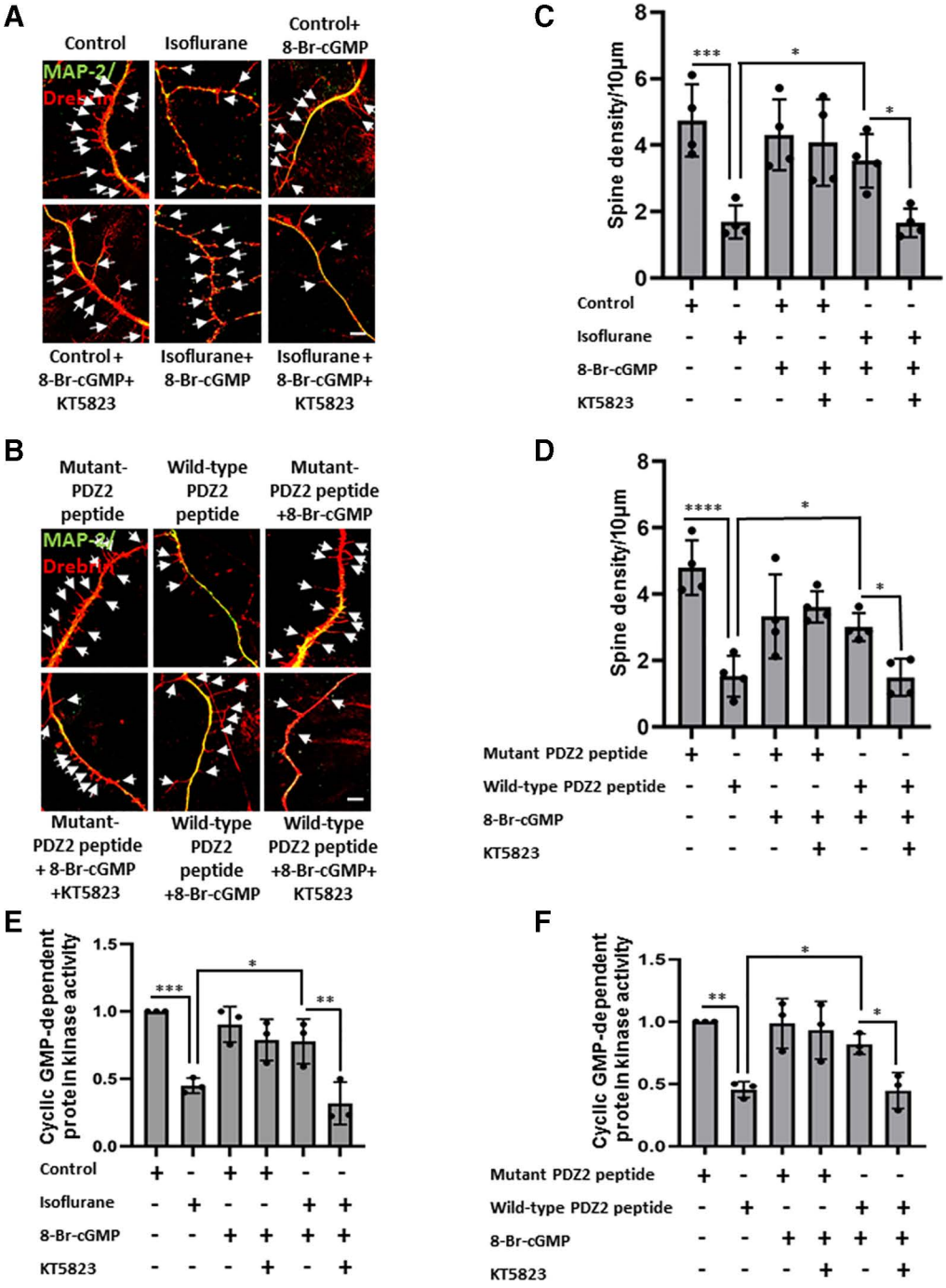

Fig. 4. Protein kinase-G inhibitor KT5823 blocked the ability of 8-Br–cyclic guanosine monophosphate (cGMP) to prevent isoflurane- and PSD-95 wild-type PDZ2 peptide–induced dendritic spine loss and decline in cGMP-dependent protein kinase activity. (*A* and *B*) Primary neuronal cells were pretreated with 8-Br–cGMP or KT5823 at the time of gas or peptides exposure and then coimmunostained for microtubule-associated protein-2 (MAP-2)/drebrin, and total spine density was calculated. Representative photomicrographs (63×) show dendritic spines in the hippocampal neurons after respective treatments; *scale bar* = 10 µm. *Arrows* indicate the dendritic spines. (*C* and *D*) Summary plots represent spine density per 10 µm dendrite length. Data were analyzed using one-way ANOVA with Bonferroni multiple comparisons test. Data represent mean ± SD; $n = 4$ independent experiments. *$P < 0.05$, ***$P < 0.001$, ****$P < 0.0001$ compared with respective control or as indicated. Hippocampal neurons were exposed to isoflurane or PSD-95 wild-type PDZ2 peptide in the presence or absence of 8-Br–cGMP or KT5823, and cGMP-dependent kinase activity was assayed. (*E* and *F*) Graphs represent the relative cGMP-dependent protein kinase activity levels after respective treatments. PSD-95 mutant PDZ2 peptide (referred to as mutant PDZ2 peptide) and PSD-95 wild-type PDZ2 peptide (as wild-type PDZ2 peptide). Data were analyzed using one-way ANOVA with Bonferroni multiple comparisons test. Data represent mean ± SD; $n = 3$ independent experiments. *$P < 0.05$, **$P < 0.01$, ***$P < 0.001$ compared with respective controls or as indicated.

cGMP-dependent protein kinase activity between control and experimental groups (mean ± SD). A decrease in the relative levels of cGMP-dependent protein kinase activity in isoflurane (0.44 ± 0.05) *versus* control, $P < 0.001$; and PSD-95 wild-type PDZ2 peptide (0.45 ± 0.06) *versus* PSD-95 mutant PDZ2 peptide, $P = 0.002$ (fig. 4, E and F). However, 8-Br–cGMP ameliorated the loss in cGMP-dependent protein kinase activity: isoflurane *versus* isoflurane + 8-Br–cGMP (0.77 ± 0.16), $P = 0.032$; and PSD-95 wild-type PDZ2 peptide *versus* PSD-95 wild-type PDZ2 peptide + 8-Br–cGMP (0.81 ± 0.08), $P = 0.037$. Conversely, adding PKG inhibitor KT5823 further decreased the cGMP-dependent protein kinase levels in the hippocampal neuronal cells: isoflurane + 8-Br–cGMP *versus* isoflurane + 8-Br–cGMP + KT5823 (0.31 ± 0.15), $P = 0.003$; isoflurane *versus* isoflurane + 8-Br–cGMP + KT5823, $P = 0.918$; PSD-95 wild-type PDZ2 peptide + 8-Br–cGMP *versus* PSD-95 wild-type PDZ2 peptide + 8-Br–cGMP + KT5823 (0.44 ± 0.14), $P = 0.033$; and PSD-95 wild-type PDZ2 peptide *versus* PSD-95 wild-type PDZ2 peptide + 8-Br–cGMP + KT5823, $P > 0.999$ (fig. 4, E and F).

Isoflurane or PSD-95 Wild-type PDZ2 Peptide–induced Loss of Synapses in Primary Neurons Is Mitigated in the Presence of 8-Br–cGMP and YC-1

Previous studies showed that isoflurane impairs synaptic plasticity in the mouse hippocampus.[40] NO-cGMP-PKG signaling is involved in the modulation of synaptic plasticity and memory formation in various brain regions.[41,42] Therefore, we first investigated effects of isoflurane or PSD-95 wild-type PDZ2 peptide on synapse in primary neurons. We exposed primary neurons with isoflurane and peptides for 4 h at 7 days *in vitro*, in the presence and absence of pharmacologic drugs of the pathway. The cells were fixed for immunocytochemistry at 14 days *in vitro*, and the concentration of all the drugs was maintained during media changes. Data were analyzed using one-way ANOVA, in which we found a significant reduction in the synaptic puncta (mean ± SD [in percentage]) in the primary neurons exposed to isoflurane (41.10 ± 14.38) in comparison to control, $P = 0.001$ (fig. 5, A and B); and PSD-95 wild-type PDZ2 peptide (50.49 ± 14.31) in comparison to PSD-95 mutant PDZ2 peptide, $P < 0.001$ (fig. 6, A and B). We next demonstrated the effects of the cGMP analog 8-Br–cGMP and YC-1 on isoflurane or PSD-95 wild-type PDZ2 peptide–induced synapse loss. Addition of 200 μM 8-Br–cGMP and 10 μM YC-1 at the time of isoflurane exposure attenuated the loss of synapse as follows: isoflurane *versus* isoflurane + 8-Br–cGMP (89.57 ± 26.98), $P = 0.011$; and isoflurane *versus* isoflurane + YC-1 (88.86 ± 29.87), $P = 0.013$ (fig. 5, A and B). 8-Br–cGMP and YC-1 also attenuated PSD-95 wild-type PDZ2 peptide–induced loss of synapse as follows: PSD-95 wild-type PDZ2 peptide *versus* PSD-95 wild-type PDZ2 peptide + 8-Br–cGMP (80.27 ± 12.04), $P = 0.045$; and PSD-95 wild-type PDZ2 peptide *versus* PSD-95 wild-type PDZ2 peptide + YC-1 (79.96 ± 9.04), $P = 0.048$, (fig. 6, A and B). Next, to validate whether activation of PKG by 8-Br–cGMP is specific and sufficient to prevent isoflurane- and PSD-95 wild-type PDZ2 peptide–induced loss in synaptic puncta, we added KT5823 along with 8-Br–cGMP. We found that KT5823 blocked the ability of 8-Br–cGMP to prevent isoflurane and PSD-95 wild-type PDZ2 peptide–induced synapse loss as follows: isoflurane + 8-Br–cGMP *versus* isoflurane + 8-Br–cGMP + KT5823 (53.42 ± 18.89), $P = 0.090$; isoflurane *versus* isoflurane + 8-Br–cGMP + KT5823, $P > 0.999$ (fig. 5, A and B); PSD-95 wild-type PDZ2 peptide + 8-Br–cGMP *versus* PSD-95 wild-type PDZ2 peptide + 8-Br–cGMP + KT5823 (60.65 ± 18.65), $P = 0.368$; and PSD-95 wild-type PDZ2 peptide *versus* PSD-95 wild-type PDZ2 peptide + 8-Br–cGMP + KT5823, $P > 0.999$ (fig. 6, A and B), indicating that this pathway is PKG-dependent.

Treatment with YC-1 Prevents Neonatal Isoflurane-induced Impairment in Object Recognition Memory in 5-week-old Mice

To determine whether neonatal isoflurane exposure or synaptic PSD-95 PDZ2 disruption contributes to cognitive impairment at later stages, we investigated the effect of isoflurane on recognition memory by assessing hippocampal-dependent object recognition at postnatal day 35 in both the male and female mice, 4 weeks after exposure at postnatal day 7. We observed that oxygen control + vehicle, oxygen control + YC-1, and isoflurane + YC-1 groups were able to discriminate between novel and known objects as calculated by significantly increased amounts of time investigating the novel object over the known object (fig. 7, A and C) mean ± SD [seconds]) for novel *versus* known: male, oxygen control + vehicle [21.36 ± 9.42 *versus* 12.07 ± 5.2], $P = 0.001$ ($n = 15$); oxygen control + YC-1 [16.12 ± 5.5 *versus* 10.12 ± 5.17], $P = 0.001$ ($n = 15$); isoflurane + YC-1 [17.62 ± 4.82 *versus* 13.16 ± 5.9], $P = 0.014$ ($n = 15$) female, oxygen control + vehicle [21.87 ± 6.5 *versus* 11.53 ± 6.62], $P < 0.0001$ ($n = 14$); oxygen control + YC-1 [19.04 ± 9.55 *versus* 11.42 ± 5.05], $P = 0.007$ ($n = 15$); isoflurane + YC-1 [18.66 ± 5.58 *versus* 13.05 ± 4.66], $P = 0.009$ ($n = 15$). In contrast, isoflurane + vehicle group depicts no significant increase in investigation time between the novel and known objects: male, isoflurane + vehicle [18.42 ± 11.69 *versus* 18.66 ± 10.1], $P = 0.940$ ($n = 15$); and female; isoflurane + vehicle [16.38 ± 4.78 *versus* 14.1 ± 4.48], $P = 0.091$ ($n = 14$), with n = number of mice. Treatment with YC-1 prevents the impairment in novel object recognition caused by isoflurane exposures as shown by the increased discrimination in novel object recognition. The discrimination or recognition index was the time investigating a novel object over the time investigating a novel object plus a familiar object × 100)[43] (fig. 7, B and D). Data were analyzed using one-way ANOVA, which indicated that the isoflurane + vehicle group performed less well than the other groups in

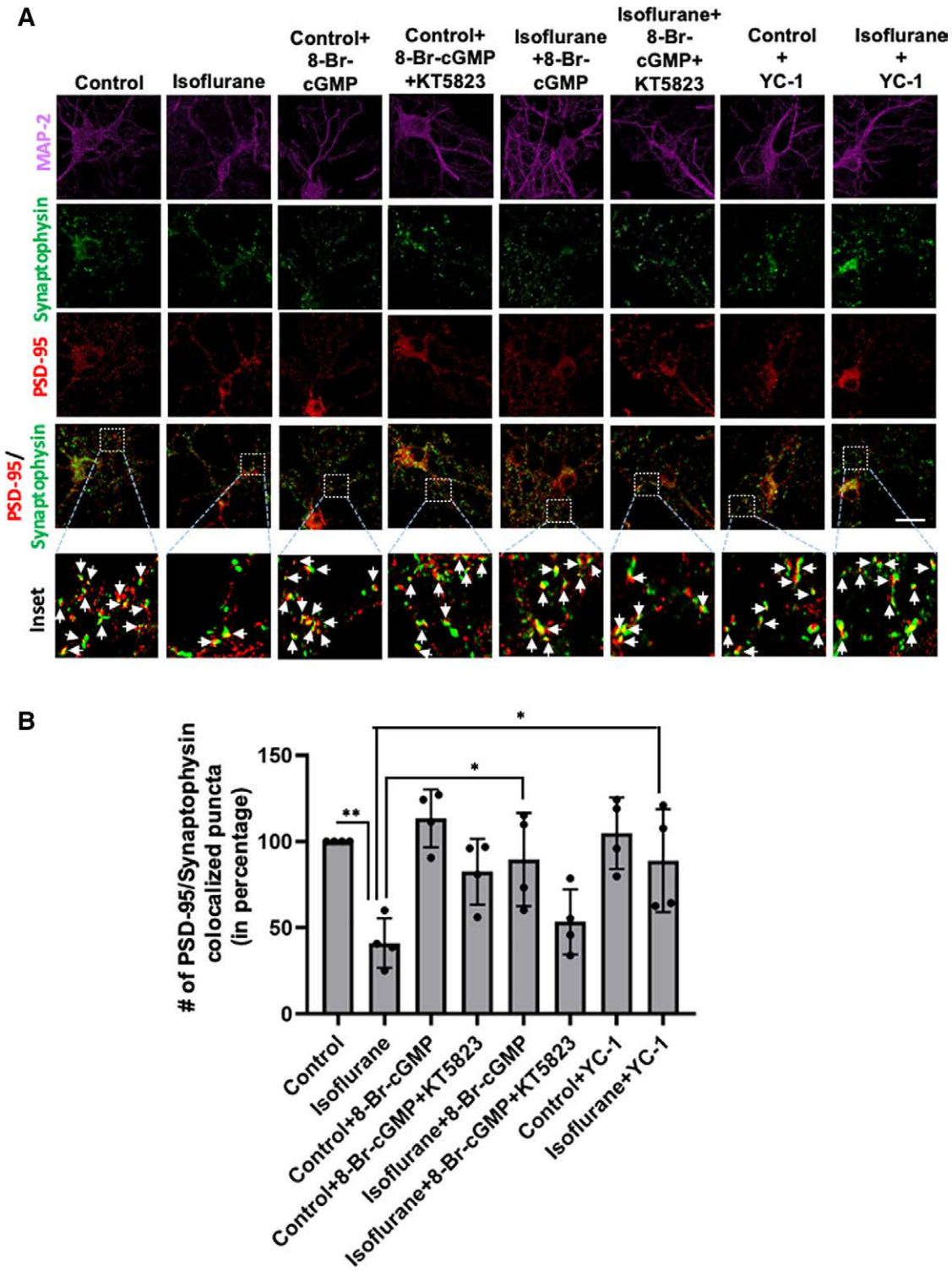

Fig. 5. 8-Br–cyclic guanosine monophosphate (cGMP) and YC-1 prevent isoflurane-induced loss in synapse, blocked in the presence of KT5823. Primary neuronal cells were pretreated with 8-Br–cGMP or YC-1 or KT5823 at the time of gas exposure. (*A*) Representative fluorescent images of primary neurons coimmunostained at 14 days *in vitro* for pre- and postsynaptic markers synaptophysin (*green*) and postsynaptic density (PSD)-95 (*red*), respectively, and microtubule-associated protein-2 (MAP-2; *magenta*). *Arrows* in the *inset* indicate the colocalized puncta of synaptophysin and PSD-95. *Scale bar* = 20 μm. (*B*) Colocalization between synaptophysin and PSD-95 was analyzed for quantification of synapses in neuronal cells. Graph represents mean ± SD (in percentage); $n = 4$ independent experiments. Data were analyzed using one-way ANOVA with Bonferroni multiple comparisons test. $^{*}P < 0.05$ and $^{**}P < 0.01$ compared with respective controls or as indicated.

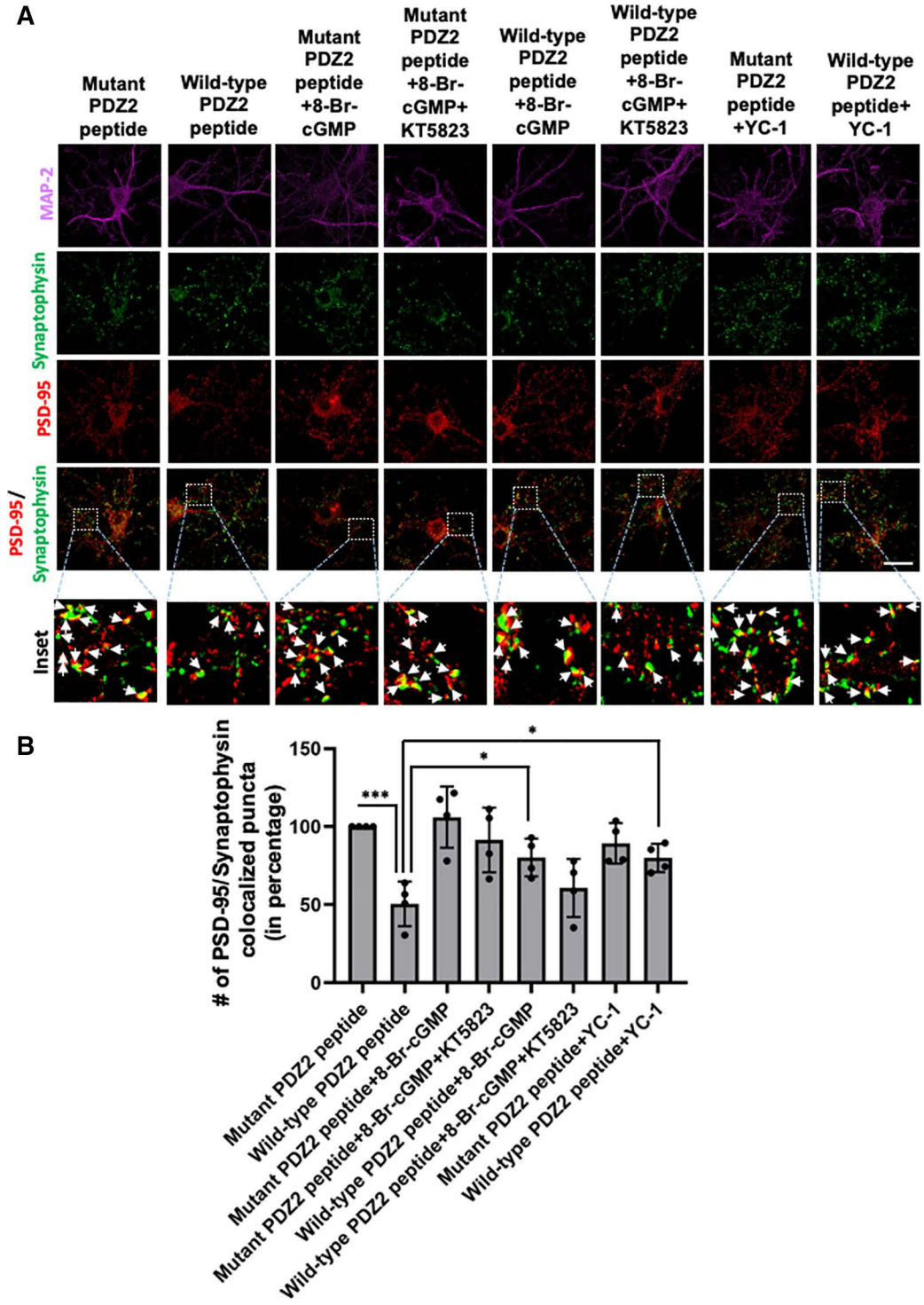

Fig. 6. Postsynaptic density (PSD)-95 wild-type PDZ2 peptide exposure causes synapse loss, which is mitigated in the presence of 8-Br–cyclic guanosine monophosphate (cGMP) and YC-1. Primary neuronal cells were pretreated with 8-Br–cGMP or YC-1 or KT5823 at the time of peptides exposure. (*A*) Representative fluorescent images of primary neurons coimmunostained at 14 days *in vitro* for pre- and postsynaptic markers synaptophysin (*green*) and PSD-95 (*red*), respectively, and microtubule-associated protein-2 (MAP-2; *magenta*). *Arrows* in the *inset* indicate the colocalized puncta of synaptophysin and PSD-95. *Scale bars* = 20 μm. (*B*) Colocalization between synaptophysin and PSD-95 was analyzed for quantification of synapses in neuronal cells. PSD-95 mutant PDZ2 peptide (referred to as mutant PDZ2 peptide) and PSD-95 wild-type PDZ2 peptide (as wild-type PDZ2 peptide). Graph represents mean ± SD (in percentage); $n = 4$ independent experiments. Data were analyzed using one-way ANOVA with Bonferroni multiple comparisons test. *$P < 0.05$ and ***$P < 0.001$ compared with respective controls or as indicated.

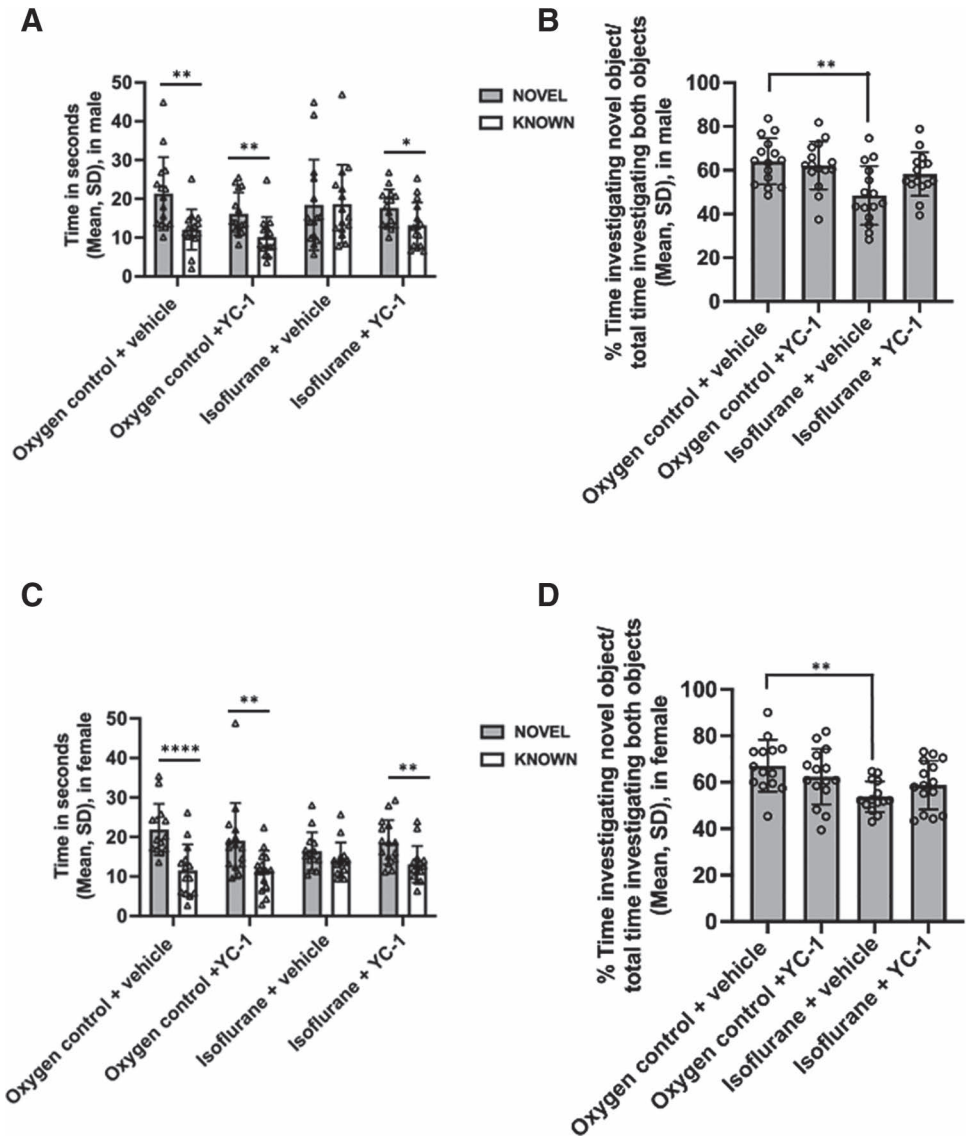

Fig. 7. Neonatal exposure to isoflurane impairs recognition memory at 5 weeks in both male and female mice. At 1 week, mice were exposed to oxygen (control) or isoflurane and were injected with YC-1 or vehicle. (*A* and *C*) Plots representing time mice spent investigating novel or known objects among experimental groups. Data are plotted as mean ± SD (seconds) for novel *versus* known: male, oxygen control + vehicle ($n = 15$), $P = 0.001$; oxygen control + YC-1 ($n = 15$), $P = 0.001$; isoflurane + YC-1 ($n = 15$), $P = 0.014$; isoflurane + vehicle ($n = 15$), $P = 0.940$, female: oxygen control + vehicle ($n = 14$), $P < 0.0001$; oxygen control + YC-1 ($n = 15$), $P = 0.007$; isoflurane + YC-1 ($n = 15$), $P = 0.009$; isoflurane + vehicle ($n = 14$), $P = 0.091$. Data were analyzed with paired *t*-test. (*B* and *D*) Plot showing recognition index as percentage of time investigating novel object/total time investigating both objects × 100; Data were analyzed using one-way ANOVA with Bonferroni multiple comparisons test. Mean recognition index ± SD: in males, oxygen control + vehicle *versus* isoflurane + vehicle, $P = 0.001$; oxygen control + vehicle *versus* oxygen control + YC-1, $P > 0.999$; oxygen control + vehicle *versus* isoflurane + YC-1, $P = 0.486$; in females, oxygen control + vehicle *versus* isoflurane + vehicle, $P = 0.003$; oxygen control + vehicle *versus* oxygen control + YC-1, $P = 0.667$; oxygen control + vehicle *versus* isoflurane + YC-1, $P = 0.100$. *$P < 0.050$, **$P < 0.01$, ****$P < 0.0001$ compared with respective controls or as indicated.

both the male and female mice (fig. 7, B and D; mean ± SD [recognition index]): males, oxygen control + vehicle [64.08 ± 10.57] *versus* isoflurane + vehicle [48.49 ± 13.41], $P = 0.001$; oxygen control + vehicle *versus* oxygen control + YC-1 [62.13 ± 10.88], $P > 0.999$; oxygen control + vehicle *versus* isoflurane + YC-1 [58.24 ± 9.99], $P = 0.486$; females: oxygen control + vehicle [67.13 ± 11.17] *versus* isoflurane + vehicle [53.76 ± 6.64], $P = 0.003$; oxygen control

+ vehicle *versus* oxygen control + YC-1 [62.4 ± 11.97], $P = 0.667$; oxygen control + vehicle *versus* isoflurane + YC-1 [58.78 ± 10.46], $P = 0.100$.

Discussion

In the current study, we examined the effects of isoflurane on synaptic PDZ2 interaction in the mouse hippocampus and on dendritic spines and synapses in the primary hippocampal neurons and cognitive functions in mice. We previously showed that inhalational anesthetics at clinically relevant concentrations disrupt PDZ domain–mediated protein–protein interactions between PSD-95 or PSD-93 and the NMDAR NR2 subunits or nNOS.[15,16,44] We speculated that disruption of synaptic PDZ2 interactions during the critical period of synaptogenesis could impair neuronal plasticity and lead to long-term cognitive dysfunction or neurologic impairments. Mostly, neurologic disorders converge into a common phenotype of impaired synaptic connectivity. We found that 4 h exposure to isoflurane or a PSD-95 wild-type PDZ2 peptide disrupted the interaction between NR2A/2B subunits and PSD-95 PDZ2 domain in the hippocampus of neonatal mouse brain. Additionally, in cultured hippocampal neurons, isoflurane and PSD-95 wild-type PDZ2 peptide caused loss of early dendritic spines, loss of mature synapses (the overlap of pre- and postsynaptic markers can be used as a representation of the mature synapse[45]), and decrease in cGMP-dependent protein kinase activity. Introduction of NO donor or cGMP analog at the time of exposure prevented the loss in early dendritic spines, mature synapses, and the decrease in cGMP-dependent protein kinase activity in response to isoflurane or PSD-95 wild-type PDZ2 peptide. Furthermore, introducing of sGC activator YC-1 in mice during the neonatal isoflurane exposure prevented the loss in object recognition memory at 5 weeks. These data suggest that dysregulation of NMDAR NR2–PSD-95–PDZ2–nNOS ternary complexes upstream after early anesthetic exposure impairs downstream components NO/sGC/cGMP–mediated PKG signaling pathway (fig. 8).

The hippocampus is the main region for learning and memory and has been implicated in the amnestic and delayed cognitive effects of anesthetics.[48] Therefore, we endeavored to understand the downstream signaling components that are perturbed in response to this disruption of synaptic PDZ2 interactions in the hippocampus. To that end, we employed primary neuronal cultures of cells dissociated from the brain hippocampus for studying the complex downstream signaling mechanisms. Previous studies from others have shown that 4 h of exposure to 1.4% isoflurane decreases dendritic filopodial spines in neonatal primary neuronal cultures at 5 days *in vitro*.[49] We explored the effects of isoflurane and PSD-95 wild-type PDZ2 peptide on dendritic spines at 7 days *in vitro* and synapse at 14 days *in vitro* since the functional polarization begins approximately a week after neuronal cells are plated. In addition, 14 days *in vitro* is a time point at which synaptic connections are well established.

We found that 4 h of isoflurane or PSD-95 wild-type PDZ2 peptide (mimics isoflurane) exposure at 7 days *in vitro* caused loss of early dendritic spines. These *in vitro* neuronal culture findings coincide with our laboratory's recently published studies in intact animals, which showed that isoflurane and PSD-95 wild-type PDZ2 peptide caused loss of spine density.[17,18] Excitatory synapses are found on dendritic spines; thus, the loss of early dendritic spines could reduce excitatory neurotransmission and also lead to loss of synapses.[50] Furthermore, we also observed that 4 h of isoflurane or PSD-95 wild-type PDZ2 peptide at 7 days *in vitro* caused a decrease in the synapses at 14 days *in vitro* in the primary neurons. Many of the PDZ domain–mediated protein–protein interactions linking the ion channels and receptors to their downstream signaling pathways have been shown to be impeded by inhalational anesthetics. The disruption of synaptic PDZ2 domains by isoflurane provides a plausible mechanism for the dissociation of the PSD-95–NMDAR–nNOS ternary complex in the neonatal brain hippocampus and cognitive dysfunctions in mice, loss of early dendritic spines, mature synapse, and cGMP-dependent protein kinase activity in the hippocampal neurons.

We next investigated whether neonatal anesthetic exposure or disruption of synaptic PSD-95 PDZ2 interactions in the hippocampus affects the memory and cognitive functions in mice once they reached a certain age. Several groups including ours have measured cognitive performance in mice using a novel object recognition behavior test that has previously indicated impairment after early exposure to anesthesia and involves hippocampal-dependent learning and memory including nonspatial recognition memory in both male and female mice.[17,18] Previously published studies from our laboratory demonstrated that 3- and 6-week-old mice exposed early to isoflurane or injected with PSD-95 wild-type PDZ2 peptide exhibited reduced recognition memory performance.[17,18] However, to validate whether this cognitive memory impairment is due to the impaired downstream sGC/cGMP-dependent signaling. We have administered sGC activator–YC-1 in mice at the time of isoflurane exposure. We found that YC-1 treatment mitigated the impairment of recognition memory in response to isoflurane, which is also similar to the findings from another group that has reported neuroprotective efficacy of YC-1 on cognitive dysfunctions in response to different anesthetics.[26] This also implicates the involvement of the sGC/cGMP–dependent signaling in early anesthetic exposure–produced cognitive impairments.

Brain development is orchestrated through the plasticity- and activity-dependent mechanisms that control spines and synapse formations and eliminations.[36] Lines of evidence suggest that activity-dependent spines and synapse formation are interceded by a postsynaptic signaling cascade implicating NO, cGMP, and vasodilator-stimulated

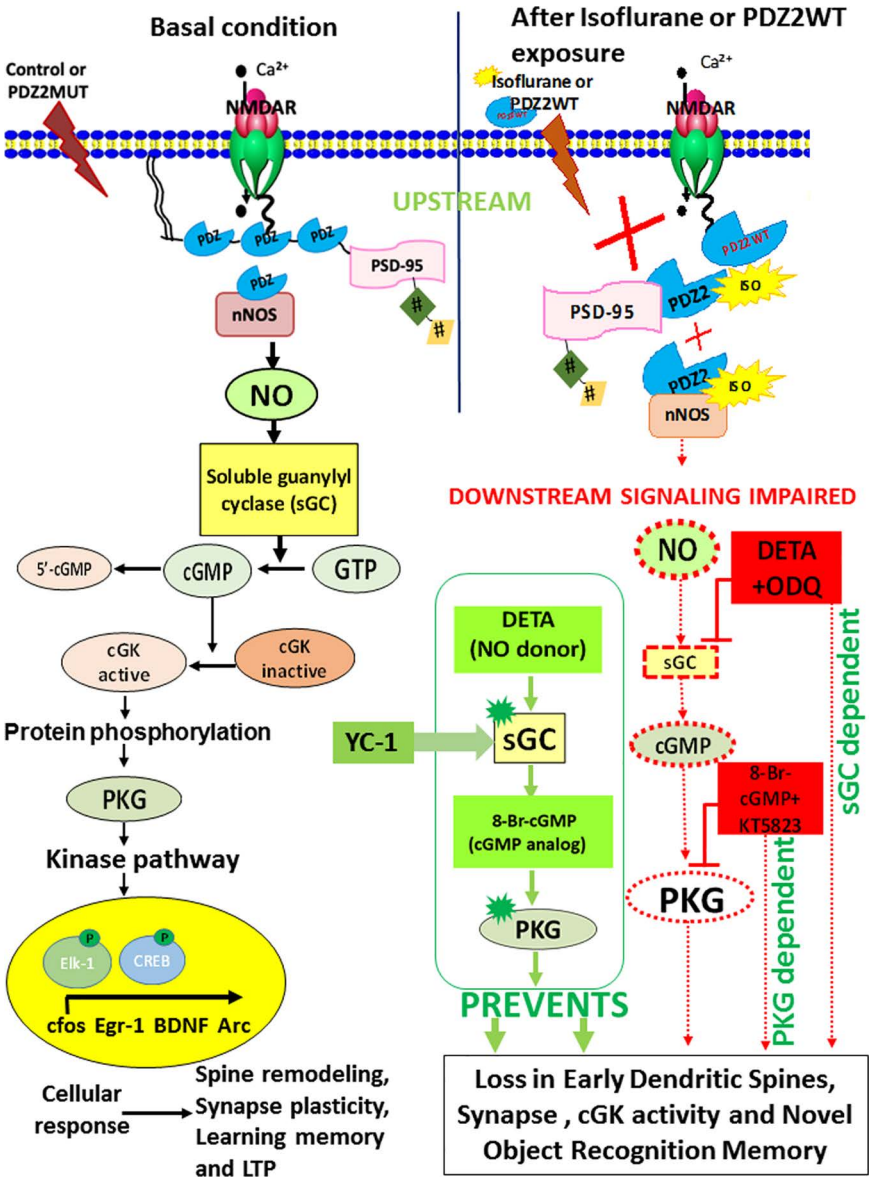

Fig. 8. Schematic representation illustrates the dissociation of *N*-methyl-d-aspartate receptor (NMDAR)–postsynaptic density (PSD)-95–neuronal NO synthase (nNOS) interaction induced by isoflurane or PSD-95 wild-type PDZ2 peptide. #To avoid complexity, not all PSD-95 family members are shown. Basal conditions: NMDAR associates with nNOS, a downstream signaling molecule, through PSD-95. Linked through its first and second PDZ domain, PSD-95 forms a ternary complex by binding to NMDAR NR2 subunit and PDZ domain in nNOS.[46] NMDAR–PSD-95/93–nNOS complexes helps Ca^{2+} influx through NMDAR on the postsynaptic membrane to activate nNOS. The NO generated is required for neuronal plasticity. It acts predominantly *via* cyclic guanosine monophosphate (cGMP) and protein kinase-G (PKG) for activation of kinase pathways. NO-independent pathways may also be activated by NMDAR. NO exerts significant control over gene expression.[47] After exposure: Exposure to inhalational anesthetics[15,16] or the intracellular addition of PSD-95 wild-type PDZ2 peptide,[19] which potentially binds to NMDAR NR2 subunits, disrupts NMDAR–PSD-95/93–nNOS complexes. This disruption can reduce the efficacy with which calcium ions activate nNOS. Pretreating neuronal cells with the NO donor DETA NONOate at the time of isoflurane or PSD-95 wild-type PDZ2 peptide exposure prevents the loss in dendritic spine density. This protection is attenuated by using soluble guanylate cyclase (sGC) inhibitor 1H-[1,2,4] oxadiazolo[4,3-a]quinoxalin-1-1 (ODQ). In the presence of ODQ, NO donor does not prevent isoflurane-induced dendritic spine loss. Additionally, pretreatment with YC-1 or 8-Br–cGMP prevents isoflurane- and PSD-95 wild-type PDZ2 peptide–induced loss of spine density or synapse. However, PKG inhibitor KT5823 blocks this prevention by 8-Br–cGMP. YC-1 treatment prevented neonatal isoflurane-mediated loss in the recognition memory in mice. *Dotted red lines* represent impaired signaling, and resulting loss in early dendritic spines, synapses, cGMP-dependent protein kinase activity, and novel object recognition memory; *green arrows* represent prevention in the presence of NO donor, sGC activator and cGMP analog. cGK, cGMP-dependent protein kinase activity; PDZ2WT, PSD-95 wild-type PDZ2 peptide.

phosphoprotein phosphorylation.[36,51] Our recent findings demonstrate that using the NO donor prevents neonatal isoflurane-induced impairments in synaptic plasticity and memory.[17] However, the pathways downstream of NO that are affected by the disruption of the synaptic PSD-95–PDZ2 domain interactions and that are responsible for the loss in early dendritic spines have not been uncovered. Therefore, to identify the downstream components of the NO-mediated signaling, we used several pharmacologic activators and inhibitors. sGC is a known receptor for NO, and its activation causes a subsequent rise in cGMP levels.[52] Here we found the components of the NO signaling pathway that sequentially activate PKG are potentially involved in the mechanisms underlying loss of early dendritic spine density and synapses in hippocampal neuronal cells in response to the isoflurane or wild-type PDZ2 peptide exposure. Pretreating the neuronal cells with NO donor DETA NONOate at the time of isoflurane and PSD-95 wild-type PDZ2 peptide exposure prevented the loss in dendritic spine density. However, this effect was reversed by using a selective sGC inhibitor (ODQ). When NO donor was added in the presence of sGC inhibitor, it did not prevent isoflurane-induced spine loss. These results implicate a role for sGC in mediating the action of NO in response to isoflurane or synaptic PSD-95 PDZ2 disruption. Hence, activation of sGC by NO is specific and sufficient to prevent isoflurane-induced dendritic spine loss in the hippocampal neuronal cells.

The NO-sGC-cGMP pathway plays an important role in modulating synaptic transmission, plasticity, and cognitive functions in the hippocampus and cerebral cortex.[53] We also observed that the effect of DETA NONOate was mimicked by the cGMP analog 8-Br–cGMP. Pretreatment of 8-Br–cGMP prevented the isoflurane- and PSD-95 wild-type PDZ2 peptide–induced loss in early spine density and synapses. To validate whether activation of PKG by cGMP is specific and sufficient to prevent isoflurane or synaptic PSD-95 PDZ2 disruption–induced spine loss, we also added 8-Br–cGMP in the presence of PKG inhibitor (KT5823) to the hippocampal neurons. However, in the presence of KT5823, 8-Br–cGMP did not prevent isoflurane-induced loss of spines. These results indicate that cGMP acts through PKG to prevent isoflurane and PSD-95 wild-type PDZ2 peptide–induced spine loss in the hippocampal neuronal cells. Furthermore, adding NO-independent sGC activator YC-1 also prevents the loss in synapse in response to isoflurane or PSD-95 wild-type PDZ2 peptide in the hippocampal neuronal cells.

Major limitations of the current study are that we have not studied the sex-specific effects in the coimmunoprecipitation and *in vitro* primary neuron culture experiments in response to the isoflurane anesthesia or PSD-95 wild-type PDZ2 peptide, given the known sex-specific sensitivity to anesthetics during distinct stages of development. Nevertheless, in response to peer review, we have performed additional experiments and have reported the sex-specific effects of neonatal isoflurane exposure in male and female mice at 5 weeks on object recognition memory (fig. 7).

Our findings show that clinically relevant concentration of isoflurane markedly disrupted the interactions between NMDAR NR2A/2B subunits and PSD-95 in the neonatal mouse brain hippocampus. We also found that neonatal isoflurane or synaptic PSD-95 PDZ2 disruption cause impairment in the recognition memory in both male and female mice at 5 weeks and loss of early dendritic spines and synapses *in vitro* without inducing significant neuronal death. Our results strongly suggest that introducing an NO donor or cGMP analog *in vitro* prevents the loss in early dendritic spines and synapses. In addition, introducing sGC activator YC-1 at the time of isoflurane exposure has prevented the loss in object recognition memory in both the sexes. Molecular dissection of these intricate mechanisms has added to our understanding of how isoflurane or disruption of the PDZ2 domain of the PSD-95 protein in the neonatal hippocampus upstream perturbs these downstream signaling pathways. Additionally, our work expands several avenues for therapeutic interventions in which targeting these molecular events might treat neurologic dysfunctions including inhalational anesthetic-related cognitive impairment.

Acknowledgments

The authors thank Claire Levine, M.S., E.L.S. (Johns Hopkins University, Baltimore, Maryland), for her excellent scientific editing.

Research Support

This work was supported by National Institutes of Health, National Institute of General Medical Sciences (Bethesda, Maryland) grant No. R01GM110674 to Dr. Johns.

Competing Interests

The authors declare no competing interests.

Correspondence

Address correspondence to Dr. Johns: Department of Anesthesiology and Critical Care Medicine, Johns Hopkins University School of Medicine, 720 Rutland Ave., Ross 361, Baltimore, Maryland 21205. rajohns@jhmi.edu.

References

1. Liu X, Ji J, Zhao GQ: General anesthesia affecting on developing brain: Evidence from animal to clinical research. J Anesth 2020; 34:765–72

2. Davidson AJ, Sun LS: Clinical evidence for any effect of anesthesia on the developing brain. Anesthesiology 2018; 128:840–53
3. Walters JL, Paule MG: Review of preclinical studies on pediatric general anesthesia-induced developmental neurotoxicity. Neurotoxicol Teratol 2017; 60:2–23
4. Lee JR, Loepke AW: Does pediatric anesthesia cause brain damage? - Addressing parental and provider concerns in light of compelling animal studies and seemingly ambivalent human data. Korean J Anesthesiol 2018; 71:255–73
5. Disma N, O'Leary JD, Loepke AW, Brambrink AM, Becke K, Clausen NG, De Graaff JC, Liu F, Hansen TG, McCann ME, Salorio CF, Soriano S, Sun LS, Szmuk P, Warner DO, Vutskits L, Davidson AJ: Anesthesia and the developing brain: A way forward for laboratory and clinical research. Paediatr Anaesth 2018; 28:758–63
6. Colon E, Bittner EA, Kussman B, McCann ME, Soriano S, Borsook D: Anesthesia, brain changes, and behavior: Insights from neural systems biology. Prog Neurobiol 2017; 153:121–60
7. Hansen TG, Henneberg SW: Neurotoxicity of anesthetic agents and the developing brain in rodents and primates: The time has come to focus on human beings. Anesthesiology 2010; 113:1244–5; author reply 1245–6
8. Maloney SE, Creeley CE, Hartman RE, Yuede CM, Zorumski CF, Jevtovic-Todorovic V, Dikranian K, Noguchi KK, Farber NB, Wozniak DF: Using animal models to evaluate the functional consequences of anesthesia during early neurodevelopment. Neurobiol Learn Mem 2019; 165:106834
9. Rappaport BA, Suresh S, Hertz S, Evers AS, Orser BA: Anesthetic neurotoxicity–Clinical implications of animal models. N Engl J Med 2015; 372:796–7
10. Bilotta F, Evered LA, Gruenbaum SE: Neurotoxicity of anesthetic drugs: An update. Curr Opin Anaesthesiol 2017; 30:452–7
11. Zeller A, Jurd R, Lambert S, Arras M, Drexler B, Grashoff C, Antkowiak B, Rudolph U: Inhibitory ligand-gated ion channels as substrates for general anesthetic actions. Handb Exp Pharmacol 2008: 31–51
12. Solt K, Forman SA: Correlating the clinical actions and molecular mechanisms of general anesthetics. Curr Opin Anaesthesiol 2007; 20:300–6
13. Jenkins A, Lobo IA, Gong D, Trudell JR, Solt K, Harris RA, Eger EI 2nd: General anesthetics have additive actions on three ligand gated ion channels. Anesth Analg 2008; 107:486–93
14. Fanning AS, Anderson JM: PDZ domains: Fundamental building blocks in the organization of protein complexes at the plasma membrane. J Clin Invest 1999; 103:767–72
15. Tao F, Chen Q, Sato Y, Skinner J, Tang P, Johns RA: Inhalational anesthetics disrupt postsynaptic density protein-95, *Drosophila* disc large tumor suppressor, and zonula occludens-1 domain protein interactions critical to action of several excitatory receptor channels related to anesthesia. Anesthesiology 2015; 122:776–86
16. Fang M, Tao YX, He F, Zhang M, Levine CF, Mao P, Tao F, Chou CL, Sadegh-Nasseri S, Johns RA: Synaptic PDZ domain-mediated protein interactions are disrupted by inhalational anesthetics. J Biol Chem 2003; 278:36669–75
17. Schaefer ML, Wang M, Perez PJ, Coca Peralta W, Xu J, Johns RA: Nitric oxide donor prevents neonatal isoflurane-induced impairments in synaptic plasticity and memory. Anesthesiology 2019; 130:247–62
18. Schaefer ML, Perez PJ, Wang M, Gray C, Krall C, Sun X, Hunter E, Skinner J, Johns RA: Neonatal isoflurane anesthesia or disruption of postsynaptic density-95 protein interactions change dendritic spine densities and cognitive function in juvenile mice. Anesthesiology 2020; 133:812–23
19. Tao F, Johns RA: Effect of disrupting *N*-methyl-D-aspartate receptor-postsynaptic density protein-95 interactions on the threshold for halothane anesthesia in mice. Anesthesiology 2008; 108:882–7
20. Kornau HC, Schenker LT, Kennedy MB, Seeburg PH: Domain interaction between NMDA receptor subunits and the postsynaptic density protein PSD-95. Science 1995; 269:1737–40
21. Nikonenko I, Boda B, Steen S, Knott G, Welker E, Muller D: PSD-95 promotes synaptogenesis and multiinnervated spine formation through nitric oxide signaling. J Cell Biol 2008; 183:1115–27
22. Penzes P, Cahill ME, Jones KA, VanLeeuwen JE, Woolfrey KM: Dendritic spine pathology in neuropsychiatric disorders. Nat Neurosci 2011; 14:285–93
23. Briner A, Nikonenko I, De Roo M, Dayer A, Muller D, Vutskits L: Developmental stage-dependent persistent impact of propofol anesthesia on dendritic spines in the rat medial prefrontal cortex. Anesthesiology 2011; 115:282–93
24. Platholi J, Herold KF, Hemmings HC Jr, Halpain S: Isoflurane reversibly destabilizes hippocampal dendritic spines by an actin-dependent mechanism. PLoS One 2014; 9:e102978
25. Yang G, Chang PC, Bekker A, Blanck TJ, Gan WB: Transient effects of anesthetics on dendritic spines and filopodia in the living mouse cortex. Anesthesiology 2011; 115:718–26
26. Yan J, Huang Y, Lu Y, Chen J, Jiang H: Repeated administration of ketamine can induce hippocampal neurodegeneration and long-term cognitive impairment via the ROS/HIF-1α pathway in developing rats. Cell Physiol Biochem 2014; 33:1715–32
27. Cao Y, Li Z, Ma L, Ni C, Li L, Yang N, Shi C, Guo X: Isoflurane-induced postoperative cognitive dysfunction is mediated by hypoxia-inducible factor-1α-dependent

neuroinflammation in aged rats. Mol Med Rep 2018;17:7730–6
28. Ippolito DM, Eroglu C: Quantifying synapses: an immunocytochemistry-based assay to quantify synapse number. J Vis Exp 2010
29. Kushwaha R, Sinha A, Makarava N, Molesworth K, Baskakov IV: Non-cell autonomous astrocyte-mediated neuronal toxicity in prion diseases. Acta Neuropathol Commun 2021; 9:22
30. Baker KB, Kim JJ: Effects of stress and hippocampal NMDA receptor antagonism on recognition memory in rats. Learn Mem 2002; 9:58–65
31. Clark RE, Zola SM, Squire LR: Impaired recognition memory in rats after damage to the hippocampus. J Neurosci 2000; 20:8853–60
32. Diwakarla S, Nylander E, Grönbladh A, Vanga SR, Khan YS, Gutiérrez-de-Terán H, Sävmarker J, Ng L, Pham V, Lundbäck T, Jenmalm-Jensen A, Svensson R, Artursson P, Zelleroth S, Engen K, Rosenström U, Larhed M, Åqvist J, Chai SY, Hallberg M: Aryl sulfonamide inhibitors of insulin-regulated aminopeptidase enhance spine density in primary hippocampal neuron cultures. ACS Chem Neurosci 2016; 7:1383–92
33. Xu J, Mathena RP, Xu M, Wang Y, Chang C, Fang Y, Zhang P, Mintz CD: Early developmental exposure to general anesthetic agents in primary neuron culture disrupts synapse formation *via* actions on the mTOR pathway. Int J Mol Sci 2018; 19:E2183
34. Xu F, Lv C, Deng Y, Liu Y, Gong Q, Shi J, Gao J: Icariside II, a PDE5 inhibitor, suppresses oxygen-glucose deprivation/reperfusion-induced primary hippocampal neuronal death through activating the PKG/CREB/BDNF/TrkB signaling pathway. Front Pharmacol 2020; 11:523
35. Coley AA, Gao WJ: PSD95: A synaptic protein implicated in schizophrenia or autism? Prog Neuropsychopharmacol Biol Psychiatry 2018; 82:187–94
36. Nikonenko I, Nikonenko A, Mendez P, Michurina TV, Enikolopov G, Muller D: Nitric oxide mediates local activity-dependent excitatory synapse development. Proc Natl Acad Sci U S A 2013; 110:E4142–51
37. Friebe A, Sandner P, Schmidtko A: cGMP: A unique 2nd messenger molecule - Recent developments in cGMP research and development. Naunyn Schmiedebergs Arch Pharmacol 2020; 393:287–302
38. Feil R, Kleppisch T: NO/cGMP-dependent modulation of synaptic transmission. Handb Exp Pharmacol 2008: 529–560
39. Arancio O, Antonova I, Gambaryan S, Lohmann SM, Wood JS, Lawrence DS, Hawkins RD: Presynaptic role of cGMP-dependent protein kinase during long-lasting potentiation. J Neurosci 2001; 21:143–9
40. Simon W, Hapfelmeier G, Kochs E, Zieglgänsberger W, Rammes G: Isoflurane blocks synaptic plasticity in the mouse hippocampus. Anesthesiology 2001; 94:1058–65
41. Chien WL, Liang KC, Teng CM, Kuo SC, Lee FY, Fu WM: Enhancement of learning behaviour by a potent nitric oxide-guanylate cyclase activator YC-1. Eur J Neurosci 2005; 21:1679–88
42. Chien WL, Liang KC, Teng CM, Kuo SC, Lee FY, Fu WM: Enhancement of long-term potentiation by a potent nitric oxide-guanylyl cyclase activator, 3-(5-hydroxymethyl-2-furyl)-1-benzyl-indazole. Mol Pharmacol 2003; 63:1322–8
43. Lueptow LM: Novel object recognition test for the investigation of learning and memory in mice. J Vis Exp 2017
44. Tao F, Su Q, Johns RA: Cell-permeable peptide Tat-PSD-95 PDZ2 inhibits chronic inflammatory pain behaviors in mice. Mol Ther 2008; 16:1776–82
45. Verstraelen P, Van Dyck M, Verschuuren M, Kashikar ND, Nuydens R, Timmermans JP, De Vos WH: Image-based profiling of synaptic connectivity in primary neuronal cell culture. Front Neurosci 2018; 12:389
46. Sattler R, Xiong Z, Lu WY, Hafner M, MacDonald JF, Tymianski M: Specific coupling of NMDA receptor activation to nitric oxide neurotoxicity by PSD-95 protein. Science 1999; 284:1845–8
47. Gallo EF, Iadecola C: Neuronal nitric oxide contributes to neuroplasticity-associated protein expression through cGMP, protein kinase G, and extracellular signal-regulated kinase. J Neurosci 2011; 31:6947–55
48. Perouansky M, Pearce RA: How we recall (or don't): The hippocampal memory machine and anesthetic amnesia. Can J Anaesth 2011; 58:157–66
49. Head BP, Patel HH, Niesman IR, Drummond JC, Roth DM, Patel PM: Inhibition of p75 neurotrophin receptor attenuates isoflurane-mediated neuronal apoptosis in the neonatal central nervous system. Anesthesiology 2009; 110:813–25
50. Tada T, Sheng M: Molecular mechanisms of dendritic spine morphogenesis. Curr Opin Neurobiol 2006; 16:95–101
51. Ota KT, Monsey MS, Wu MS, Schafe GE: Synaptic plasticity and NO-cGMP-PKG signaling regulate pre- and postsynaptic alterations at rat lateral amygdala synapses following fear conditioning. PLoS One 2010; 5:e11236
52. Wykes V, Bellamy TC, Garthwaite J: Kinetics of nitric oxide-cyclic GMP signalling in CNS cells and its possible regulation by cyclic GMP. J Neurochem 2002; 83:37–47
53. Zhihui Q: Modulating nitric oxide signaling in the CNS for Alzheimer's disease therapy. Future Med Chem 2013; 5:1451–68